

ANFIS-FUZZY LOGIC BASED UPQC IN INTERCONNECTED MICROGRID
DISTRIBUTION SYSTEMS: MODELLING, SIMULATION AND IMPLEMENTATION

A Dissertation by

Udaya Kishan Renduchintala

Master of Technology, GITAM University, India, 2011

Bachelor of Technology, Jawaharlal Nehru Technological University, India, 2008

Submitted to the Department of Electrical Engineering and Computer Science
and the faculty of the Graduate School of
Wichita State University
in partial fulfillment of
the requirements for the degree of
Doctor of Philosophy

December 2020

© Copyright 2020 by Udaya Kishan Renduchintala

All Rights Reserved

ANFIS-FUZZY LOGIC BASED UPQC IN INTERCONNECTED MICROGRID
DISTRIBUTION SYSTEMS: MODELLING, SIMULATION AND IMPLEMENTATION

The following faculty members have examined the final copy of this dissertation for form and content and recommend that it be accepted in partial fulfillment of the requirement for the degree of Doctor of Philosophy, with a major in Electrical Engineering and Computer Science.

Chengzong Pang, Committee Chair

M. Edwin Sawan, Committee Member

Ward T. Jewell, Committee Member

Aravinthan Visvakumar, Committee Member

Krishna Krishnan, Committee Member

Accepted for the College of Engineering

Dennis Livesay, Dean

Accepted for the Graduate School

Coleen Pugh, Dean

DEDICATION

To my parents, my brother, my life partner,
and my dear friends

ACKNOWLEDGMENTS

I would like to thank my adviser, Dr. Chengzong Pang, for his many years of guidance and support. His motivation has helped me to expand the horizons of this project. I sincerely extend my thanks to Dr. M. Edwin Sawan, Dr. Ward T. Jewell, Dr. Visvakumar Aravinthan, Dr. Krishna Krishnan, for their cooperation and support.

I wish to express my profound sense of respect and gratitude to George Massey, Hitek Inc. for his constant support, thoughtful supervision and encouragement through this research project. I want to extend my heartfelt thanks to Patrick Rorabaugh, Hitek Inc. for his help in building the prototype circuit. Thanks are also due to Shocker I-Corps and Hitek Inc. for providing funding to this research work.

I wish to express my sincere thanks to Krishna Mohan Tatikonda for contributing remotely from India to this project.

Finally, I want to express my indebtedness to Mohana Turaka, my life partner for having unshakable belief in me throughout my PhD education.

ABSTRACT

This study focuses on the improvement of the power quality in interconnected power distribution systems using connected microgrids. The power quality issues at the secondary distribution level are addressed using a unified power quality conditioner (UPQC), which aids in controlling voltage imbalances and current harmonics. Further, a power control method, adaptive neuro-fuzzy inference system (ANFIS), is proposed as a global solution by installing independent compensating devices at the point of common coupling. The proposed strategy can improve the power quality in traditional installations because the proposed UPQC method maximizes power utilization and improves the efficiency of the system. The microgrids integrate renewable energy sources, which generate green energy with low loss. Case studies, a prototype, and simulations via MATLAB/Simulink are used to validate the proposed method, and the results prove the enhancement in power quality control. The proposed control strategy had a response time of 0.3 s, reduced peak voltage distortions, and restored the voltage at the interconnecting point to a normal level. The total harmonic distortion of currents decreased from 21.13% to 14.74% when a PI technique was used to control the UPQC-P, and the proposed ANFIS-based UPQC-P reduced the harmonic content to 2.43% from 21.13%.

TABLE OF CONTENTS

Chapter	Page
1. INTRODUCTION	1
2. LITERATURE REVIEW	5
2.1 Power Flow Control.....	6
2.2 Voltage Control.....	8
2.3 Power Quality Improvement.....	8
2.4 Power System Stability Improvement	9
2.5 Grid Interactions	10
2.6 In Distribution Systems.....	10
2.7 Testing of FACTS Devices.....	11
3. MOTIVATION FOR IMPROVEMENTS TO UPQC.....	16
3.1 Selection of UPQC.....	17
3.1.1 Based on Topology	17
3.1.2 Based on the Type of Inverter.....	19
3.1.3 Based on the Supply.....	19
3.1.4 Based on the Method of Control.....	19
3.2 Determination and Characterization of UPQC for this Project	20
4. CONTROL SYSTEM DESIGN WITH ANFIS	25
4.1 UPQC-P-DVR Control	25
4.1.1 DVR Control Objectives.....	25
4.1.2 Implementation	25
4.2 UPQC-P-DSTATCOM Control.....	27
4.2.1 DSTATCOM Control Objectives:	27
4.2.2 Implementation	28
4.3 Design of UPQC	29
4.3.1 Selection of DC bus voltage:	30
4.3.2 Selection of DC bus capacitor:	30
4.3.3 Selection of AC inductor:	31
4.3.4 Selection of ripple filter:	31
4.3.5 Voltage and Current ratings of IGBTs:.....	31
4.4 Fuzzy Logic Controller	32
4.4.1 Fuzzification Module	32
4.4.2 Constructing Membership Functions	33
4.4.3 Fuzzy Inference System.....	35
4.4.4 Defuzzification.....	36
4.4.5 Analysis.....	37
4.5 Neural Networks	39

TABLE OF CONTENTS (continued)

Chapter	Page
4.5.1	Algorithm for Neuro Controller:..... 41
4.5.2	Advantages of Neural Networks: 41
4.6	ANFIS Acclimation 43
4.6.1	Creating a Sugeno System 44
4.6.2	Know your Data..... 44
4.6.3	Implementation 45
5.	SIMULATION AND RESULTS..... 49
5.1	Voltage and Power magnitudes 50
5.1.1	Three-Phase-to-Ground Fault (LLL): 50
5.1.2	Single-Phase-to-Ground Fault (LG): 51
5.1.3	Double-Phase-to-Ground Fault (LLG): 53
5.2	Voltage and Current waveforms 54
5.3	FFT Analysis..... 56
5.3.1	Case 1: Without any Controller 57
5.3.2	Case 1: With PI Controller..... 57
5.3.3	Case 2: With fuzzy controller 58
5.3.4	Case 3: With ANFIS controller..... 58
5.4	Experimental Validation 59
5.4.1	Schematic Design..... 59
5.4.2	Prototype Design..... 60
5.4.3	Experimental Results 61
6.	CONCLUSIONS..... 65
	REFERENCES 67

LIST OF TABLES

Table		Page
1.	Table 1 Switching Pattern for Series and Shunt Inverters	47
2.	Table 2 UPQC Prototype Parameters	64

LIST OF FIGURES

Figure	Page
1. Typical Interconnected System.....	13
2. Right Shunt UPQC.....	18
3. Left Shunt UPQC.....	18
4. Constructional Structure of a UPQC.....	21
5. (a) Voltage injected by the DVR in sag condition, (b) Voltage absorbed by the DVR in swell condition	23
6. Control Diagram Implementation.	27
7. Membership Function for input voltage	34
8. Membership Function for output.	37
9. Mapping fuzzy logic inputs and output.	37
10. Overview of Fuzzy Logic Controller.	38
11. Flow chart of control flow to generate PWM signals.	39
12. Multilayer Feedforward Network	40
13. Mapping ANFIS inputs and output.....	43
14. Mapping ANFIS inputs and output.....	45
15. Overview of ANFIS Controller.	46
16. Waveforms of three-phase inverter corresponding to the PWM signal.....	46
17. Real-time implementation of the ANFIS control system.	48
18. Test System with UPQC connected.....	49
19. Sag magnitudes with a three-phase fault at feeder 4.....	51
20. Reduced sag magnitudes with the application of the UPQC at feeder 4.	51
21. Voltage and power magnitudes during a fault condition at feeder 12.	52
22. Effect of ANFIS UPQC-P connected at feeder 12 after the fault.	52

LIST OF FIGURES (continued)

Figure	Page
23. Line to line fault at feeder 14.....	53
24. Reduced spikes in voltage under UPQC-P at feeder 14.	54
25. PCC voltage under fault condition.....	55
26. Injected voltage by the DVR.....	55
27. Pollutant free voltages at PCC.	55
28. Harmonic content in source currents.	56
29. Injected current by the DSTATCOM.	56
30. Pollutant free currents at the consumer load end.	56
31. THD of load currents without any controller.....	57
32. THD of load currents with PI controller.	58
33. THD of load currents with Fuzzy controller.	58
34. THD of load currents with ANFIS controller.	59
35. Control diagram schematic for VSIs.....	60
36. Experimental setup with the prototype UPQC-P.....	61
37. Grid voltage under fault condition.....	62
38. Injected voltage by the UPQC.	62
39. Pure voltages at PCC.	62
40. Harmonics in source currents.....	63
41. Injected current by UPQC.....	63
42. Clean load end currents.....	63
43. THD comparison for load currents with different controllers.	65

CHAPTER 1

INTRODUCTION

Although most power systems throughout the industrialized world started as small-scale isolated systems, they eventually expanded and became interconnected, leading to large-scale centralized electricity generation and transmission. Denial of the inexorability of macrogrids emerged in the late 1960s as researchers began to study the added benefits of increased centralization. It was predicted these benefits would diminish with larger grids or even provide higher efficiency for the currently existing large grids [1], [2].

The electric power system (EPS) consists of the area EPS and the local EPS. The area EPS consists of generation, transmission, sub-transmission, and distribution systems. Central station plants generate most electricity at voltages up to 30 kV, and generator step-up transformers at the plant substation raise the voltage to greater levels to power the transmission system. Transmission facilities generally are greater than 34 kV or 69 kV, and sub-transmission systems typically range from 34.5 kV to 69 kV. Distribution systems are in the 15 kV range and include distribution substations; the primary voltage circuits supplied by these substations; distribution transformers; secondary circuits, including services to customer premises; and circuit-protection, voltage-regulation, and control devices. EPS is mandated to satisfy several requirements, including service, reliability, security, quality, and cost-effectiveness. EPS also must meet numerous technical performance requirements parameters such as voltage, frequency, power quality, and fault duty. There is no universally binding requirement to make the EPS more accommodating for DR interconnection. The local EPS consists of distribution and facility equipment on the customer's side of the point of common coupling [3]. In the 1990s and 2000s, failures in large-scale grids in the United States and Europe led to a cascading effect. They caused widespread, economically

damaging blackouts, and the need for reliable decentralized power systems became apparent. In recent years, researchers have analyzed ways to optimize small-scale power systems, including the use of microgrids. Microgrids are localized groupings or aggregations of small-scale generators; they may differ in their size, efficiency, or type of connection to the main grid. Interconnected microgrid systems have two modes of operation. One is called interconnected or grid-connected mode, where the microgrid and main grid are physically connected and synchronized to work collaboratively to achieve the demand side targets. The second mode, called islanding mode, describes a condition in which a segment of the grid is temporarily isolated from the main grid; it remains powered by its own distributed generation resources [3]–[6]. Microgrids are considered viable options for those places where main grid expansion is either impossible or has no economic justification, such as the electrification in university campuses, military installations, and rural villages [4]. Some researchers regard the microgrid as a specific distribution system embedded with distributed generations, which may operate in grid-connected or islanded (stand-alone) mode [2]. Even though there are some common characteristics between the distribution system and microgrid, for example, voltage level and customer types, microgrid has its unique structure. The microgrid consists of renewable sources, backup generators, energy storage, unbalanced load demand on each phase, and multiphase lines. This unique structure, both grid-connected mode and stand-alone mode, as one of the most critical microgrid features, can deliver power whether there is a power outage on the grid side.

Along with this beneficial advantage, there are potential challenges to keep the system running safely and well. One of the main concerns in the microgrid study is the electrical power quality issue. From massive amounts of experience, it is essential to assess electrical power quality for the sake of devices and users. For example, it has been reported that a 10% increase in voltage

stress caused by harmonic current typically results in a 7% increase in the operating temperature of a capacitor bank and can reduce its life expectancy by 30% [4].

Harmonics study becomes significant for researchers to save the life of electric devices and provide more reliable power to customers. Scholars who study the power system used to ignore the inside functioning process of components in the large system since what the output brings are far more critical. However, the situation is different. Because of the integration of renewable energy, the output of electrical sources is not conventional. Aiming to understand the output of renewable energy sources, looking into each component's detailed model can be a solution. Significantly, the photovoltaic source is often integrated into local low voltage level microgrids and should be studied. Given the small scale of loads and generation in micro-grid, the number of harmonics produced by PV will cause more significant influences than conventional large grids, such as overheating electronic devices, low power quality, and loss of power. Apparently, not just consumers but also utility companies would like to find a solution to minimize those negative influences. However, before researchers can actually find a solution for this problem, how to model, analyze, and quantify harmonics in microgrids should be accomplished first.

Alternating current (AC) power, started in 1886 in North America, is the primary form in the electrical grid system. It operates in a sinusoidal waveform to transfer electric power. In the United States, the frequency of it is 60 Hz. According to its own characteristic, every electronic device connected to AC power is designed to function well under clean electric power. Clean power means whether voltage or current only contains components in 60 Hz. However, recent advances in technology have made the question of AC power quality even more important [4]. Human beings have been using coal as a source of electric power for over a hundred years, and the pollution it brought to our society has alerted governments around the world. To reduce

pollution, green and renewable energy is considered as one of the solutions. In a single day, enough sun shines in China meet its energy needs for more than ten years, at least theoretically [5]. Massive potential development stimulates both researchers and utilities working on integrating renewable energy into the established power system. Yet challenges are coming along with potential benefits. Different origins can cause the same results. While innovative electric devices, for example, personal computers, have induced concerns on power quality, renewable energy integration leads to some negative influences on power quality. Electric Power Quality (EPQ) is a term that refers to maintaining the near sinusoidal waveform of power distribution bus voltages and currents at the rated magnitude and frequency [5].

CHAPTER 2

LITERATURE REVIEW

FACTS devices are based on power electronics and are used to improve electric power transmission systems in steady-state and transient state conditions [6]. FACTS devices also help increase transmission lines power transfer capacity [6]. The ability of an alternating current (AC) transmission line to transfer AC electric power is constrained by various factors, including the thermal limit, voltage limit, transient stability limit, and short circuit current limit. These limits define the maximum power, called the power transfer capability, which can be transferred through the AC transmission line without damage to the transmission line and the electrical equipment. A FACTS device provides control of one or more parameters of an AC transmission system. These parameters include the voltage magnitude, voltage angle, and the impedance of the transmission line. Through these parameters' control, the FACTS device can control the real and reactive power flow, the voltage magnitude, and the shunt reactive power compensation. There are four different types of FACTS [6]:

1. **Series devices.** These are variable impedance devices that inject voltage in a series with the transmission line. Depending on the phase angle between the injected voltage and the line current, they can help control the real and reactive power. Examples of series devices include a thyristor-controlled series capacitor (TCSC), thyristor switched series capacitor (TSSC), and static synchronous series compensator (SSSC).
2. **Shunt devices.** These are variable impedance devices that inject current at the point of connection. Depending on the phase angle between the injected current and the line voltage, these devices can control the real and reactive power. Examples of shunt devices include SVC and STATCOM.

3. Series-series devices. These are a combination of series devices, where each series device provides series compensation for each line and transfers active power among the transmission lines. An example of such a device is the interline power flow controller (IPFC).
4. Shunt-series devices. These are a combination of series and shunt devices, which are controlled in a coordinated way. An example of such a device is the UPFC, which is the most versatile among all FACTS devices. It can selectively or concurrently handle the real and reactive power flow via the transmission line, the bus voltage magnitude, and reactive power compensation [7].

The research works are reviewed below for each one of the different grid services offered by FACTS.

2.1 Power Flow Control

The split TCSC provides better power flow control services than the single TCSC [8]. An adaptive TSSC with discrete non-linear control provides power flow control and improves power system transient stability [9]. An SSSC with an oscillation damping controller simultaneously achieves power flow control and low-frequency oscillation damping in a system with a wind farm [10]. The modular multi-level converter-based UPFC regulates the power system's power flow in steady-state and transient state conditions [11]. A hybrid UPFC, composed of a smaller capacity UPFC and a larger capacity Sen transformer, provides the same services of active and reactive power flow control, with the advantage of much lower installation costs [12]. A method for the optimum location of TCSC relieves congestion in both the normal state and contingency state with a single line outage [13]. An analytical method determines the optimum location of the TCSC and SSSC and relieves congestion in both the normal state and contingency state with a single line fault [14]. A pricing-based method finds the optimum location of the UPFC that mitigates line

congestion and minimizes system operation costs [15]. A sensitivity-based optimization method finds the optimum place and rated capacity of the UPFC that minimizes congestion costs [16]. Reactive power dispatch (RPD) is a grid service that simultaneously minimizes reactive power flow in lines, total active power loss in transmission lines, and voltage deviation in buses. The optimal allocation of four TCSCs and three SVCs at the IEEE 30 bus system significantly reduces the total reactive power flow in lines [17]. The optimal reactive power allocation of three different FACTS, namely TCSC, SVC, and thyristor-controlled phase angle regulator (TCPAR), shows that an SVC is slightly better in improving the voltage profile. Simultaneously, a TCPAR is better in reducing the total active power loss [18]. Compared with the case without a UPFC, the optimal allocation of one UPFC provides a more significant reduction of transmission lines total active power loss and buses' voltage deviation for both the IEEE 57-bus and the IEEE 118-bus test systems [19]. In an AC-DC power system with 96 AC buses and two DC terminals, the optimal allocation of one UPFC, under contingency conditions, significantly impacts the minimization of power loss and voltage deviation [20]. The available transfer capability (ATC) measures the interconnected power system's ability to transfer electric power from one power system to another through the transmission lines. The increase of ATC is significant because it helps transfer low-cost energy to the loads.

FACTS devices can increase the ATC by redistributing power flows. The optimal allocation of one UPFC increases the ATC for the IEEE reliability test system and a 196-bus power system in North America [21]. Since series FACTSs help increase the ATC, it is proposed that these devices should be simultaneously optimized with power generation in a market environment [22]. The UPFC provides a higher increase of the ATC in comparison to STATCOM and SSSC [23] and comparison to an SVC and thyristor-controlled phase shifter (TCPS) [24]. The optimal

allocation of multiple FACTS, namely TCSC, TCPS, SVC, and UPFC, provides a significant increase in the ATC [25]. Several research works have shown that FACTS devices reduce total active power loss. An optimally allocated UPFC is more effective than an optimally allocated TCSC to minimize load curtailment on IEEE 14-bus and IEEE 30-bus test systems [26]. Wind power curtailment is minimized by an optimally allocated TCSC [27] and an optimally allocated distributed power flow controller [28]. An optimally allocated SVC is more effective than an optimally allocated TCSC to minimize wind power curtailment [29]. The combined optimal allocation of SVC and TCSC significantly reduces wind power curtailment [30].

2.2 Voltage Control

The SVC's voltage control capability was investigated, and a reactive power dispatch model was developed that restores the SVC operating point and regulates the bus voltage [31]. A photovoltaic inverter is controlled as a STATCOM and provides voltage control in power distribution systems [32]. The limits of the UPFC were included in a steady-state power flow model, which was validated by simulations that highlight the capabilities of a UPFC for coordinated voltage control and power flow control [33]. An optimization methodology was developed to identify the optimal parameter settings of one UPFC and manage to relieve voltage violations and overloads caused by line outages [34]. A probabilistic methodology improved the steady-state bus voltage profile by optimally sizing the TCSC, STATCOM, and UPFC [35].

2.3 Power Quality Improvement

FACTS devices, such as SVC, STATCOM, and UPFC, offer significant power quality services to the grid, including enhancing the power system reliability and mitigation of voltage sags, harmonics, and unbalance [36]. The capability of the SVC, STATCOM, and dynamic voltage restorer (DVR) to mitigate voltage sags, harmonics, and unbalance was shown in [37]. Distribution STATCOM and SVC minimize voltage sags and the economic losses in power distribution

systems [38]. SVC, STATCOM, and DVR reduce losses due to voltage sags [39]. An appropriate control strategy allows the UPFC to provide harmonic isolation in non-linear loads [39].

2.4 Power System Stability Improvement

A non-linear control method of STATCOM was developed for damping inter-area oscillations, which was validated on a power system with 16 generators and 68 buses [40]. A single FACTS device successfully damps inter-area oscillations and intra-area (local) oscillations [41]. The STATCOM provides robust damping of inter-area oscillations at different load conditions [42]. The coordinated control of STATCOM and generator excitation achieves transient stability and voltage regulation [43]. Hardware in the loop validation verified the transient stability enhancement obtained by a wide-area controlled SVC [44]. STATCOM, in combination with energy storage systems, enhances the transient stability of power systems with induction generators and synchronous generators [45]. STATCOM offers vast improvement of first swing transient stability [46]. The coordinated use of SSSC, TCSC, and STATCOM improved a power system's transient stability with photovoltaics and wind farms [47]. Eigen-value analysis or modal analysis can be applied to identify buses (locations) sensitive to voltage collapse and buses where power injections are the most beneficial. The modal analysis identifies the optimum location of SVC for voltage support [48]. Optimally allocated UPFCs enhance power system voltage stability under single outage contingency criterion [49]. The optimal coordinated allocation of SVCs and TCSCs enhance security against voltage collapse by keeping bus voltages and ensuring voltage stability margins [50]–[52]. In the case of low loads or low voltages, regarding voltage stability, the SSSC is superior to the controllable series compensator (CSC) [53]. An analytical method was used to estimate CSC's efficiency, SSSC, SVC, and STATCOM for voltage stability enhancement [54].

2.5 Grid Interactions

The coordinated use of multi-type FACTS devices offers multiple grid services [55]. The multiple grid services are mathematically formulated as multi-objective optimization problems. An optimally allocated UPFC simultaneously minimizes total active power loss and maximizes power system predictability in systems with a high wind power penetration [55]. In these systems, predicting the system state is very difficult due to wind power generation uncertainties. An optimally allocated UPFC simultaneously minimizes transmission line total active power loss and maximizes the voltage stability limit [56]. The best results are obtained when the transformer taps are optimized in combination with optimizing the UPFC location and parameter settings. Optimally allocated TCSCs and SVCs simultaneously minimize the total active power loss, minimize load voltage deviation, and maximize the static voltage stability margin, considering single outage contingency criteria, line thermal limits, and bus voltage limits [57]. An optimally allocated hybrid flow controller (HFC), phase shifting transformer (PST), and maximize power system loading ability [58]. The HFC provides better results in comparison with PST. Optimally allocated TCSC, SVC simultaneously minimize total active power loss, and minimize system operation cost, including the cost of FACTS, the energy loss cost, and the congestion cost [59]. The FACTS location, size, and parameter settings are optimized in combination with existing reactive power sources.

2.6 In Distribution Systems

Many techniques have been proposed for siting of FACTS devices, but only a few have compared them with other methods. A study is needed to compare techniques in speed and accuracy. The majority of the study is on the radial distribution network. Still, as increasing reliability of interconnected distribution networks is essential, the study must consider the interconnected distribution network for FACTS and DGs' siting. Most authors have focused on the

single network; for the study, multiple FACTS and multiple DGs allocation must be done for having an idea of real distribution networks. Total harmonic distortion is a major issue in power quality. Only a few authors have focused on this field, so power quality should also be the researcher's objectives to improve system performance. Much of the research work is based on balanced distribution networks; behavior of optimally placed FACTS and DGs must also be discussed in unbalanced distribution systems. Protection is a key for maintaining a stable power system; none of the reviewed literature focused on security; a broad research field is open on this topic. Most of the research is on DSTATCOM, other FACTS devices should also be optimally placed, and discussion on the behavior should be given with economic analysis. Hybrid techniques are used for future research work in planning, operation, and optimal placement, for enhancing the performance of power networks. Consideration of microgrids and virtual power plants in the context of DG planning with FACTS devices, aiming at multi-objective optimization, needs to be investigated [60].

2.7 Testing of FACTS Devices

The testing of distributed energy resource inverters according to ancillary service requirements has been well established recently. Several standards and guidelines are in place, stating requirements and respective testing procedures [60]. Factory testing occurs at the manufacturer's facilities, compliance testing at independent accredited institutes, and, finally, commissioning testing occurs in the field. On the other hand, FACTS testing is more challenging due to its high rating and large size. For example, the typical capacities of recent transmission STATCOMs applied in the USA are 100 to 200 MVAR with some large units reaching 250 MVAR, while SVCs can have powered up to 500 to 600 MVAR [61].

For this reason, most of the studies on FACTS perform digital simulations, while fewer involve laboratory or field tests. In practice, digital simulations (e.g., transient stability, dynamic

performance) are used for the functional specification of a FACTS device, which refers to the definition of equipment requirements, typically performed by the buyer (typically the TSO) or a consultant [61]. IEEE 1031: 2011 [62] proposes an approach to prepare a specification for a transmission SVC using conventional thyristor technology, which can be partly used for STATCOM and other devices. The guide describes newer developments in SVC component equipment and control systems and SVC applications' latest practices, among other topics. Similarly, IEEE P1052/08 [63] aims to assist users in specifying the functional requirements for transmission STATCOMs, using forced commutated technology based on voltage source converter topologies. The guide covers specifications, applications, engineering studies, main component characteristics, system functions, and features, factory testing, commissioning, and STATCOM systems operations. It addresses the following functions: Reactive power compensation, voltage regulation and control, transient and dynamic stability, and control and protection. The manufacturing of the device, based on the specification, is followed by factory testing at the manufacturer's facilities. This includes the testing of the valves as the most critical component. Standards for the testing of valves are IEC 61954:2011 [64] for the thyristors of SVCs and IEC 62927:2017 [65] for voltage source converter valves of STATCOMs. More specifically, IEC 61954:2011 defines the type, production, and optional tests on thyristor valves used in thyristor controlled reactors, thyristor switched reactors, and thyristor switched capacitors, forming part of SVCs [60]. Insulation tests aim to verify that the valve design meets the requirements specified (e.g., dielectric and operational tests). Production tests aim to demonstrate proper manufacturing (e.g., voltage check), and optional tests are added to the type and production tests (e.g., voltage transient test). IEC 62927:2017 applies to self-commutated valves for use in voltage source converters for STATCOMs. It includes type tests (e.g., dielectric, operational, and

electromagnetic interference tests) and production tests (e.g., voltage withstand check) for air-insulated valves. Moreover, according to their respective standards, the manufacturer also tests all other FACTS device components (e.g., transformer, circuit breakers, etc.). Particular attention needs to be paid to the control system's testing, including dynamic performance tests and protection system tests [60].

One of the vital functions among interconnected power systems is maintaining a smooth transition when switching from the main grid to microgrid when entering islanding mode. The major goal of this work is to design a device with this unique, controlling action. Figure 1 shows a typical interconnected system. As interconnected power systems require the integration of various energy sources, power quality problems, such as abnormal fluctuations in voltages and frequency and increases in harmonic content in the current, are major concerns that have been studied in recent research. For instance, the quality and stability of power produced by microgrids in bus systems are of interest as distribution systems have multiple feeders and require power for numerous sensitive electronic devices [66].

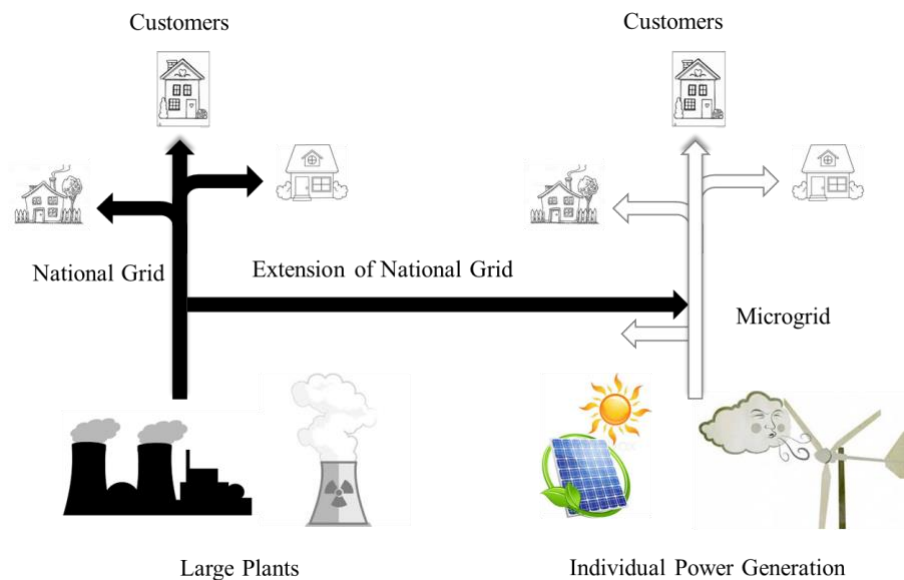


Figure 1. Typical Interconnected System

However, the control of active and reactive power transfers is not focussed on in the above-cited works. Unified power quality conditioner (UPQC), constructed on p-q theory principles, is widely used for mitigating fluctuations in power and compensates reactive power harmonics and current and voltage harmonics [67]. However, it has only been applied to single-phase systems. Owing to the dynamic nature of the elements present in UPQC, stability problems arise when three single-phase devices are paralleled to get a three-phase UPQC [68], [69]. Several local solutions to power fluctuation have been studied recently, including grid assistance, harmonic current compensation, and ride through capability during voltage sags [70], [71]; however, these have not been scaled up to provide a global solution.

Additionally, a new control strategy has been designed for voltage source inverters based on the neuro-fuzzy technique [72]. Driven by the work done in the preceding references and to overcome their limitations, in this paper, an integrated energy system is considered, and a global solution is proposed to address all of the existing power quality problems at the distribution level. The proposed UPQC can be compared to the other FACTS devices in terms of performance, features, reliability, and cost. The static variable compensator (SVC) is an essential device used to compensate for reactive power using a Thyristor Switched Capacitor – Thyristor Controlled Reactor (TSC-TCR). This is a more standard, flexible device, and it requires a smaller rating of the reactor, consequently, generates fewer harmonics. However, it is only limited to reactive power compensation and cannot handle any voltage shortcomings, switching transients, etc. STATCOM is another popular device used to manage reactive power flow without any passive elements, which can absorb or generate reactive power. But it cannot handle voltage sags and swells. The proposed UPQC will address the switching transients on the inverter side, voltage imbalances, harmonics, minimized switching losses at low cost.

A review of the recent research shows the necessity for an integrated controller between the utility grid and the distributed energy resources at the load end to enhance output and maintain the balance in the overall system. Thus far, many control techniques have been proposed involving UPQC; the work described here is a combination of acclaimed schemes focused on improving the control schema of a microgrid, including the following goals.

1. Power quality maintenance at the distribution end while switching from grid-connected mode to islanding mode.
2. Compensation of voltage sags and swells in grid voltages.
3. Real and reactive power control in both grid-connected mode and isolated mode.

The organization of this thesis is as follows: chapter 3 explains the core structure of UPQC and its selection among several UPQC configurations; the control system design and implementation based on Fuzzy Logic and ANFIS are explored in chapter 4; results based on MATLAB/Simulink simulations are explained in chapter 5, and chapter 6 includes the conclusions and references.

CHAPTER 3

MOTIVATION FOR IMPROVEMENTS TO UPQC

A unified power quality conditioner (UPQC) is a device that is similar in construction to a unified power flow conditioner (UPFC) [73]. The UPQC, like a UPFC, employs two voltage source inverters (VSIs) connected to a common dc energy storage capacitor. One of these two VSIs is connected in series with the ac line, while the other is connected in shunt with the same line. A UPFC is employed in a power transmission system to perform shunt and series compensation simultaneously. Similarly, a UPQC can also perform both tasks in a power distribution system. However, at this point, the similarities in the operating principles of these two devices end. Since a power transmission line generally operates in a balanced, distortion-free environment, a UPFC must only provide balanced shunt or series compensation [73].

On the other hand, a power distribution system may contain unbalance, distortion, and harmonic components. Therefore, a UPQC must operate under this environment while providing shunt or series compensation. The UPQC is a relatively new device, and not much work has been reported on it yet. It has been viewed as a combination of series and shunt active filters in [73]. In [73], it has been shown that it can attenuate current harmonics by inserting a series voltage proportional to the line current. Alternatively, the inserted series voltage is added to the voltage at the point of common coupling. The device can provide a buffer to eliminate any voltage dip or flicker. It is also possible to operate it as a combination of these two modes. In either case, the shunt device is used for providing a path for the real power to flow to aid the operation of the series-connected VSI. Also included in this structure is a shunt passive filter to which all the relatively low-frequency harmonics are directed. Experimental results with a relatively stiff voltage source are also provided in [73].

The motivation for developing this multipurpose custom power device is to address various aspects of power quality. The main types of power quality concerns include minimizing load harmonics, VAR/reactive power compensation, and voltage sag/swell mitigation. A controller or device would address these problems with a fast, dynamic response and steady-state accuracy. Such a controller installed on the distribution side would potentially serve as a global solution for all of the issues mentioned above associated with power quality. Therefore, it is expected that the UPQC described here will become one of the most powerful solutions for dealing with power quality problems about microgrids. The UPQC in this study is a combined shunt and series custom power device, built by connecting two voltage source inverters (VSIs) back-to-back, which is bridged by a shared DC-link capacitor for exchanging real and reactive powers [73]. The DSTATCOM is the shunt device connected in parallel to the load side and administers load balance, supplies reactive power compensation, and eliminates harmonic content. The DVR is connected in series with the supply system via an injection transformer and protects the consumer loads from voltage fluctuations. When these sags and swells occur, the DVR restores the voltage to a predetermined reference voltage level. In other words, the UPQC is an integration of the DSTATCOM and the DVR [73].

3.1 Selection of UPQC

A UPQC can be categorized by the type of the topology (right shunt, left shunt, or interline), the type of inverter used (VSI or current source inverter (CSI)), supply based (two-wire, three-wire, or four-wire), and the kind of compensation (UPQC-P, UPQC-Q, or UPQC-S).

3.1.1 Based on Topology

Right shunt, left shunt, or interline are three different topologies, classified based on the position of DVR and DSTATCOM to the distribution bus system. Figure 2 shows a right shunt UPQC will have DVR connected in series with the AC mains using a matching transformer to

mitigate sag, swell, spikes, and notches to balance and regulate the terminal voltage across the consumer loads to eliminate the voltage harmonics. It has been used to eliminate negative sequence voltages and to regulate the load voltages in three-phase systems. Electric utility companies can install it to compensate voltage harmonics and damp out harmonic propagation caused by resonance with line impedances and passive shunt compensators.

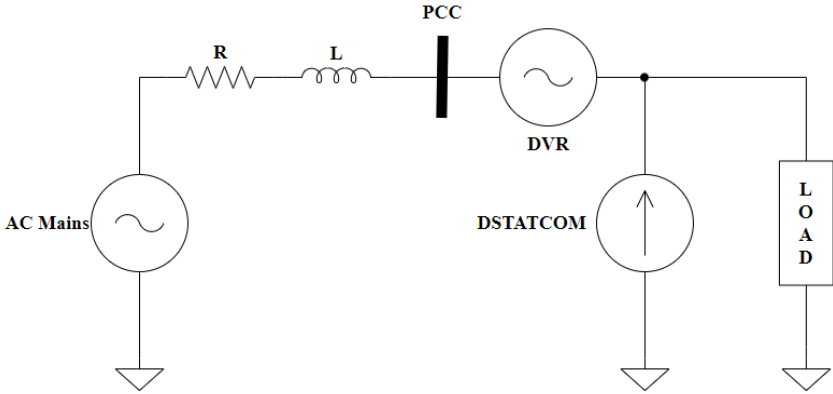


Figure 2. Right Shunt UPQC

DSTATCOM is connected in shunt with the critical loads. Figure 3 shows a left shunt UPQC configuration has its DSTATCOM connected in shunt with the AC mains, DVR connected in series with the sensitive loads. Its main drawbacks are high cost and complexity control.

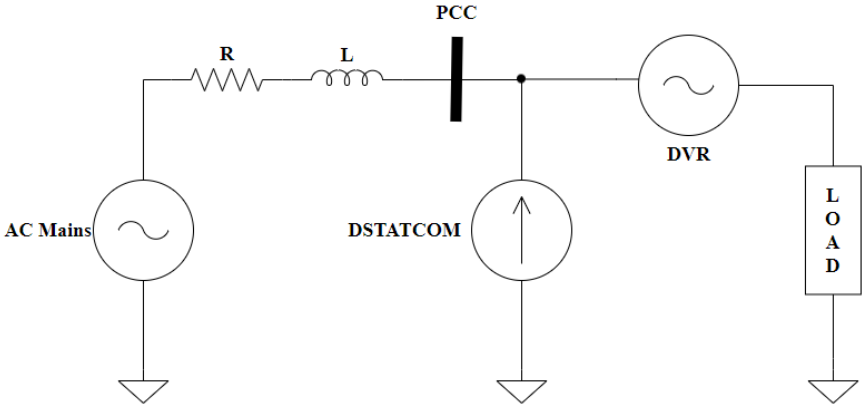


Figure 3. Left Shunt UPQC

Interline UPQC is generally connected between two individual feeders and serves a different purpose.

3.1.2 Based on the Type of Inverter

Two types of inverters are used in the development of UPQCs, VSI and CSI. VSI based UPQCs have many advantages over CSI based UPQCs. In CSIs, a diode is used in series with the self-commutating device, IGBT, in this case for reverse voltage blocking. The CSI UPQCs are considered sufficiently reliable but have higher losses and require higher inductive energy storage values at DC bus, making the overall design bulky, noisy, costly contributing to high losses. CSIs cannot be applied to multi-level inverters because of their pulsated format output.

3.1.3 Based on the Supply

UPQCs may also be classified according to the supply systems as single-phase two-wire UPQCs, three-phase three-wire UPQCs, and three-phase four-wire UPQCs. There are many consumer loads, such as domestic appliances connected to single-phase supply systems, some three-phase consumer loads without a neutral terminal, such as from three-wire supply systems.

3.1.4 Based on the Method of Control

UPQCs can be classified based on the method of control. UPQC-P: A DVR is used for series voltage injection in phase with supply current with only an active power injection. In this type of UPQC, the DVR rating is relatively low as it requires minimum series voltage injection. This type of operation is entirely satisfactory for both voltage sag and swell compensation. UPQC-Q: A DVR is used for series voltage injection in quadrature with supply current with almost zero active power injection. The DVR cannot compensate for voltage swell in the UPQC-Q mode of operation. The DSTATCOM compensates the reactive power of the consumer load, and a unity power factor is realized at PCC. This mode is considered the most conservative and provides a

minimum level of compensation. UPQC-S: A DVR is used for series voltage injection at an optimum phase angle with minimum KVA rating, S. In a UPQC-S, the shunt compensator DSTATCOM is used for all current based compensation other than full reactive power of load at the load end. In such situations, the series compensator DVR injects a voltage in series between the AC mains and the load end at a predetermined phase angle with PCC voltage. It needs both the active power and reactive power throughout the series VSI with a minimum VA rating of both VSIs.

3.2 Determination and Characterization of UPQC for this Project

In this case study, an IEEE 30 bus system is used along with a three-wire UPQC. The three single-phase injecting transformers of the DVR side are connected in series with the distribution feeder in delta-star winding, as shown in Figure 1. Similarly, the connections of the step-down transformer that feeds the load are also in delta-star winding. While selecting the type of UPQC, though the CSI-based UPQCs are reliable, they demand large inductance values for energy storage at the DC bus, making the system bulky and expensive. Therefore, a VSI-based UPQC is preferable.

Furthermore, a right shunt UPQC has its DVR connected to the supply system in series before the load, and the DSTATCOM is in shunt to the load side. Electric utility companies prefer this right shunt UPQC configuration at the distribution side to compensate for voltage and current harmonics. Left shunt UPQCs and interline UPQCs have a high implementation cost and require complex control systems. Consequently, the right shunt UPQC has a preferable design as it has lower ratings for both of the inverters and does not require complex control. Additionally, the UPQC-P type is preferable to the UPQC-Q and the UPQC-S because of its lower power rating. It has a better ability to mitigate voltage sag and swell problems. Considering all possible factors

related to the classifications of UPQCs, a three-wire, VSI-based, right shunt UPQC-P was selected for this study as shown in Figure 4 below.

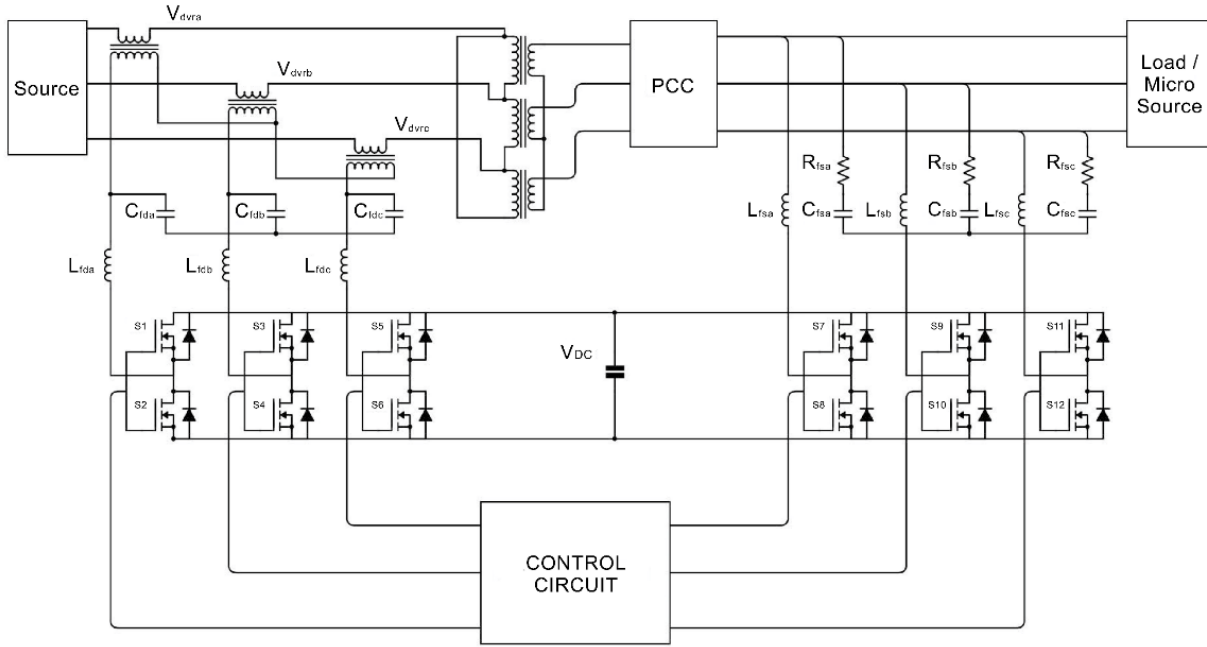


Figure 4. Constructional Structure of a UPQC

Let us now characterize the operation of UPQC by injection of voltage and current to the load. Let us assume that the load and source are unbalanced. From the right shunt UPQC structure, it can be observed that the $v_t + v_d = v_l$. If the source voltage is unbalanced, the terminal voltage will also be unbalanced. Therefore, to obtain the balanced voltage at the load terminal, v_d must cancel out the unbalanced voltage at the terminal side.

$$V_{d0} = -V_{t0}, V_{d2} = -V_{t2} \quad (1)$$

The above condition designates that V_l is a strictly positive sequence. Let us assume that the magnitude of positive sequence voltage is $|V_{l1}|$. Note that the angle of this voltage will depend on the power factor of the load. The injected positive sequence voltage is now generated such that the series compensator does not require any positive sequence power. The source current i_s flowing through the series compensator can be observed here. This yields the following equation.

$$V_{t1} + |V_{d1}| (a_1 + jb_1) = V_{l1} \quad (2)$$

Where $a_1 + jb_1$ is a unit vector that is 90° to I_{s1} . Assuming $V_{l1} = |V_{l1}| \angle 0^\circ$ the following equation is derived.

$$V_{d1}^2 - 2a_1|V_{l1}||V_{d1}| + V_{l1}^2 - V_{t1}^2 = 0 \quad (3)$$

As in the case of DVR, if the desired voltage level $|V_{l1}|$ is achievable the quadratic equation shown above has two positive real solutions of $|V_{d1}|$. The minimum of these two solutions will be chosen and requires less support from the UPQC. For the shunt current injection, by applying KCL at the entering node, we get $i_s + i_f = i_l$. Therefore, the shunt compensator must inject current to cancel the zero and negative sequences of load current. Thus, we get

$$I_{f0} = I_{l0}; I_{f1} = 0; I_{f2} = I_{l2} \quad (4)$$

This will ensure that a purely positive sequence current equals the positive sequence load current I_{l1} flows through the source. Therefore, both unbalance in the source voltages and load currents are canceled by the right shunt UPQC.

In this experimental setup, the pulse width modulation (PWM) technique was used in both VSIs to control the output voltage. The DVR side inverter was operated under PWM voltage-controlled mode to inject and absorb voltages. The inverter pertaining to DSTATCOM was operated under PWM current-controlled mode to inject required currents to the consumer loads. As PWM techniques require high-frequency switching, the inverter design requires ripple filters. The instantaneous source voltages, load voltages, and load currents were monitored by Hall effect sensors and used as feedback signals. The required control algorithm, which is discussed below, was implemented pragmatically with a digital signal processor (DSP), where the required gating signals for the insulated-gate bipolar transistors (IGBTs) were generated. Reference signals for both of these VSIs can be determined with the guidance of several control algorithms, as mentioned

in the literature review [73]. Control algorithms are classified into two types: time domain and frequency domain. After a detailed analysis of the contemporary methods, synchronous reference frame theory (SRFT), a time-domain algorithm, was selected as a basis for the work presented here. Figure 5(a), 5(b) shows the phasors for the DVR part of the UPQC-P. The voltage sag or swell can be expressed as

$$V_{sag/swell} = |V_{LC} - V_S|/V_{LC} = V_{DVR}/V_{LC} \quad (5)$$

where $V_{sag/swell}$ is the amount of voltage sag or swell required to compensate, which is usually 30% of the rated value. V_{LC} is the compensated load voltage V_S is the supply voltage; and V_{DVR} is the voltage injected by DVR.

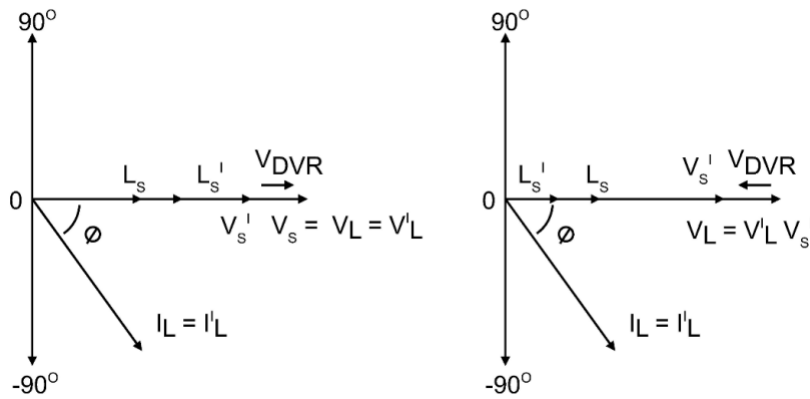


Figure 5. (a) Voltage injected by the DVR in sag condition, (b) Voltage absorbed by the DVR in swell condition

Voltage injected by the DVR is given by

$$V_{DVR} = V_{LC} - V_S \quad (6)$$

The DVR rating in kVA is given by

$$S_{DVR} = V_{DVR}I_S = V_{LC}I_L \cos \phi \quad (7)$$

where I_S is the supply current, I_L is the load current, and $\cos \phi$ is the power factor of the load.

Likewise, DSTATCOM current is given by

$$I_{DST} = \sqrt{(I_L^2 - I_S^2) + (V_{sag/swell} I_L \cos^2 \theta)} \quad (8)$$

The DSTATCOM rating in kVA is given by

$$S_{DST} = V_{LC} I_{DST} \quad (9)$$

Therefore, the overall rating of UPQC is

$$S_{UPQC} = S_{DVR} + S_{DST} \quad (10)$$

There are several factors to consider when designing or evaluating the converters' control systems to maintain the overall system's stability and power output. These include the controller's robustness, the algorithm of the controller, choice of the control signal, and the controller's location.

CHAPTER 4

CONTROL SYSTEM DESIGN WITH ANFIS

This chapter will justify the use of SRFT in controlling both of the VSIs of the UPQC in this study. This algorithm was selected after carefully following the contemporary reference signal-generating techniques, and the experimental setup implements through a signal conditioning board and a microprocessor.

4.1 UPQC-P-DVR Control

4.1.1 DVR Control Objectives

The series-connected converter has the following control objectives [74]:

1. To balance the voltages at the load bus by injecting negative and zero sequence voltages to compensate for those present in the source.
2. To isolate the load bus from harmonics, present in the source voltages, by injecting the harmonic voltages.
3. To regulate the magnitude of the load bus voltage by injecting the required active and reactive components depending on the power factor on the source side.
4. To control the power factor at the input port of the UPQC (where the source is connected).

Note that the shunt converter controls the power factor at the output port of the UPQC (connected to the load).

4.1.2 Implementation

In accordance with SRFT for generating reference signals, the hall effect sensors sense both supply voltages (V_{sa}, V_{sb}, V_{sc}) and load terminal voltages (V_{La}, V_{Lb}, V_{Lc}) in order to derive gating signals for the IGBTs of the series inverter. Reference values for both the inverters are derived and compared with the actual sensed values, as shown in Figure 6. Then, the values for

voltage and current that need to be injected are determined. For the series VSI, the reference voltages are sourced from the three-phase voltages (V_{sa}, V_{sb}, V_{sc}) that are at the point of common coupling (PCC). Hall effect sensors are used to sense these voltages, and the sensed voltages go through a signal conditioning board, which consists of a difference amplifier, a set of resistors and capacitors to step down the voltage that is suitable for a microcontroller and a DSP to implement the abc to d-q-0 transformation. The signal conditioning board also consists of a bandpass filter (BPF) to eliminate ripple contents before their transformation. A first-order Butterworth filter was used to perform this function. The DSP TMS320F28335 and Xilinx 3XCS1000 FPGA were programmed to complete this action. The d-axis and q-axis voltages are expressed as

$$V_{sd} = v_{dDC} + \tilde{v}_{dAC} \quad (11)$$

$$V_{sq} = v_{qDC} + \tilde{v}_{qAC} \quad (12)$$

The ripple voltages are described by (7) and (8). These ripple voltages can be eliminated by processing the voltages through a low pass filter (LPF) to obtain v_{dDC} and v_{qDC} . A PI controller is used to maintain the amplitude of the load terminal voltage (V_L) to its reference level (V_L^*). The calculation of the amplitude of the AC load terminal voltage (V_L) is given by (9).

$$V_L = \sqrt{\frac{2}{3}(v_{La}^2 + v_{Lb}^2 + v_{Lc}^2)} \quad (13)$$

The reference load voltage values of the d-axis, q-axis are

$$v_d^* = v_{dDC} \quad (14)$$

$$v_q^* = v_{qDC} + v_{qr} \quad (15)$$

where v_{qr} is the output of the PI controller as shown in Figure 6, which is used for regulating the voltage at PCC. The summation of q-axis voltages v_{qDC} and v_{qr} is constituted as the v_q^* as shown in (11). The d-q components, obtained from (10) and (11), undergo transformation to get abc

quantities, where the $\cos \theta$ and $\sin \theta$ angles are accessed through the three-phase phase-locked loop (PLL) function and serve as reference load voltages ($V_{La}^*, V_{Lb}^*, V_{Lc}^*$). Therefore, the amount of voltage that needs to be injected by the voltage inverter can be calculated using (12). The difference between the reference load voltages ($V_{La}^*, V_{Lb}^*, V_{Lc}^*$) and the sensed load voltages (V_{La}, V_{Lb}, V_{Lc}) are calculated with the use of a comparator:

$$\begin{bmatrix} V_{dvra} \\ V_{dvrb} \\ V_{dvrc} \end{bmatrix} = \begin{bmatrix} V_{La}^* \\ V_{Lb}^* \\ V_{Lc}^* \end{bmatrix} - \begin{bmatrix} V_{La} \\ V_{Lb} \\ V_{Lc} \end{bmatrix} \quad (16)$$

As the voltages required to be injected in series are acquired from (12), the inverter's PWM gating signals are configured accurately with the help of a Fuzzy/ANFIS controller.

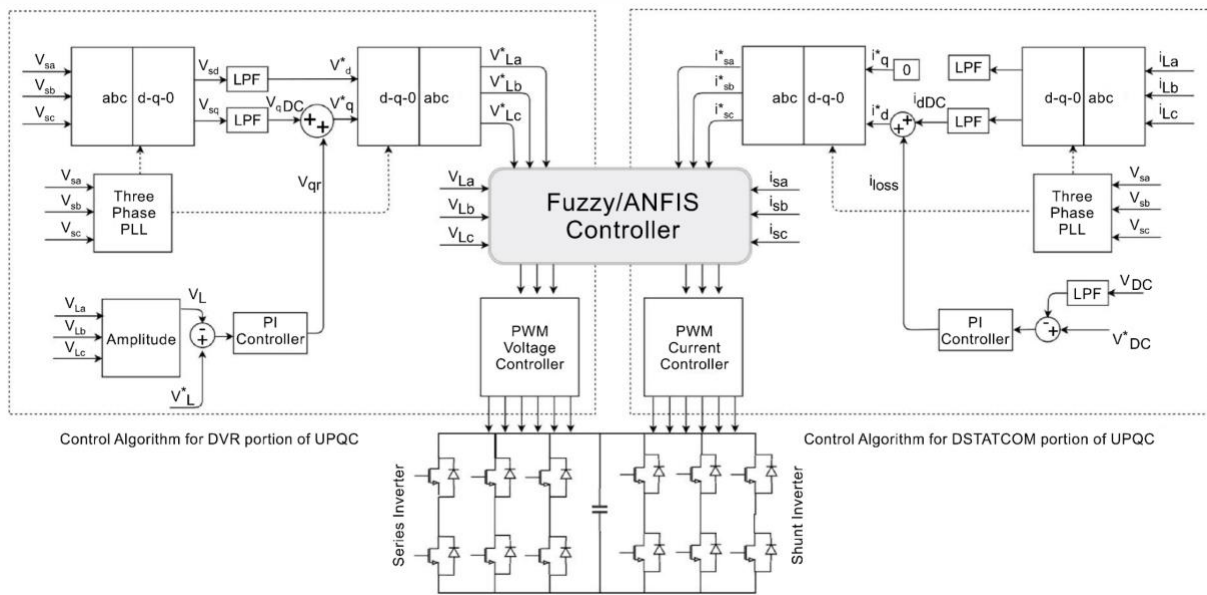


Figure 6. Control Diagram Implementation.

4.2 UPQC-P-DSTATCOM Control

4.2.1 DSTATCOM Control Objectives:

The shunt connected converter has the following control objectives [74]:

1. To balance the source currents by injecting negative and zero sequence components required by the load.

2. They compensate for the harmonics in the load current by injecting the required harmonic currents.
3. To control the power factor by injecting the required reactive current.
4. To regulate the DC bus voltage.

4.2.2 Implementation

In the control scheme of DSTATCOM, it is necessary to sense the load currents (i_{La}, i_{Lb}, i_{Lc}), PCC voltages (V_{sa}, V_{sb}, V_{sc}) and DC bus voltage (V_{DC}) to derive the gating signals for the IGBTs of the shunt inverter. In this case, the hall effect sensors were used to sense the instantaneous load currents, passed through a signal conditioning board, and fed to the microcontroller and the DSP. The load currents were transformed from abc to d-q-0 frame as

$$\begin{bmatrix} i_{Ld} \\ i_{Lq} \\ i_{L0} \end{bmatrix} = \frac{2}{3} \begin{bmatrix} \cos \theta & -\sin \theta \\ \cos \left(\theta - \frac{2\pi}{3} \right) & -\sin \left(\theta - \frac{2\pi}{3} \right) \\ \cos \left(\theta + \frac{2\pi}{3} \right) & \sin \left(\theta + \frac{2\pi}{3} \right) \end{bmatrix} \begin{bmatrix} \frac{1}{2} \\ \frac{1}{2} \\ \frac{1}{2} \end{bmatrix} \begin{bmatrix} i_{La} \\ i_{Lb} \\ i_{Lc} \end{bmatrix} \quad (17)$$

where $\cos \theta$ and $\sin \theta$ are obtained using a PLL method from PCC voltages. The d-axis and q-axis currents are expressed as

$$i_{Ld} = i_{dDC} + i_{dAC} \quad (18)$$

$$i_{Lq} = i_{qDC} + i_{qAC} \quad (19)$$

As mentioned earlier, (14) and (15) show DC and ripple contents passed through an LPF to obtain the reference signals. A PI controller at the DC bus voltage was employed to keep up the DC bus voltage and meet the losses, and the output of the PI controller gives the current component (i_{loss}) for meeting its losses. Hence, reference supply current amplitude is given by

$$i_d^* = i_{DC} + i_{loss} \quad (20)$$

As shown in Figure 6, the resultant d-q-0 currents are converted back into abc frame to obtain the reference supply currents (i_{sa}, i_{sb}, i_{sc}) using the reverse park's transformation by acquiring the needed $\cos \theta, \sin \theta$ values from the PCC voltages using a three-phase PLL function. The difference between the reference supply currents ($i_{sa}^*, i_{sb}^*, i_{sc}^*$) and the sensed supply currents (i_{sa}, i_{sb}, i_{sc}) are calculated with the use of a comparator and given by

$$\begin{bmatrix} I_{stata} \\ I_{statb} \\ I_{statc} \end{bmatrix} = \begin{bmatrix} i_{sa}^* \\ i_{sb}^* \\ i_{sc}^* \end{bmatrix} - \begin{bmatrix} i_{sa} \\ i_{sb} \\ i_{sc} \end{bmatrix} \quad (21)$$

As the currents that are required to be injected in the shunt are acquired from (17); these are sent to the current-controlled PWM inverter and are configured accurately with the help of a fuzzy logic controller. Both the control circuits for generating gating signals are realized by Adaptive Neuro Fuzzy Inference Systems based circuits. In the early stages of this project, fuzzy logic alone is considered to have control on the required voltage and current components. Later, it is extended using ANFIS to make real-time adaptation possible. Before dwelling on the design of this control structure, a fundamental understanding of fuzzy logic is required. It consists of the theory of fuzzy sets which relates to classes of objects with round boundaries in which membership is a matter of degree [21]. The reason for selecting a fuzzy controller for this project is its ability to deal with uncertainty.

4.3 Design of UPQC

The design of UPQC includes a detailed analysis for deriving the design equations for calculating the values of different components used in their circuit configurations. The three-phase three-wire UPQC is considered in this work and explained here step by step. It includes the design of VSI and its other passive components. The UPQC includes a VSI, interfacing inductors, and a ripple filter. A ripple filter is used to filter the switching ripples from the voltage at PCC. The

interfacing inductors and a ripple filter are carried out to limit the ripple in the currents and voltages. The design also includes the DC bus voltage level, DC bus capacitance, and the rating of switches. The design of DC bus capacitor depends on the energy storage capacity needed during the transient conditions. The rating of the UPQC depends on the required reactive power compensation and degree of unbalance in the load. Hence the current rating of the UPQC is affected by the load power rating, and its voltage rating is dependent on DC bus voltage. A three-leg VSI is used as a distribution static compensator, and this topology has six IGBTs, three AC inductors, and a DC capacitor. The required compensation to be provided by the UPQC decides the rating of the VSI components. The VSI is designed for compensating power of 10KVA in a 230V, 50Hz, three-phase distribution system for MATLAB simulation.

4.3.1 Selection of DC bus voltage:

The minimum DC bus voltage of the UPQC VSI should be greater than twice the peak of the distribution system's phase voltage. The DC bus voltage is calculated as

$$V_{DC} = 2\sqrt{2}V_{LL}/\sqrt{3}m \quad (22)$$

where m is the modulation index and is considered as 1, V_{LL} is the AC line output voltage of UPQC. Thus V_{DC} is obtained as 375.58V for a V_{LL} of 230V and is selected as 400V.

The main objective of the control algorithm of UPQC is to estimate the reference currents using feedback signals. These reference currents and the sensed currents are used in PWM current-controlled VSI to derive PWM gating signals for the switching devices.

4.3.2 Selection of DC bus capacitor:

The value of the DC capacitor C_{DC} of the UPQC VSI depends on the instantaneous energy available to the UPQC during the transients. The principle of energy conservation is applied as

$$\frac{1}{2} C_{DC} (V_{DC}^2 - V_{DC1}^2) = 3kVIat \quad (23)$$

Where V_{DC} is the nominal DC voltage equal to the reference DC voltage and V_{DC1} is the minimum voltage level of the DC bus, a is the overloading factor, V is the phase voltage, I is the phase current, and t is the time by which the DC bus voltage is to be recovered.

Considering the minimum voltage level of the DC bus V_{DC1} 653.20V, $V_{DC} = 700V$, $V = 240V$, $I = 75A$, $t = 30msec$, $a = 1.2$ and variation of energy during dynamics = 10%. The calculated value of C_{DC} is approximately 13000 μ F.

4.3.3 Selection of AC inductor:

The selection of AC inductance L_r of a UPQC VSI depends on the current ripple I_{crp} switching frequency f_s and DC bus voltage V_{DC} and is given as $L_r = \sqrt{3}mV_{DC}/12f_s aI_{crp}$

Where m is the modulation index, and a is the overloading factor. Considering the ripple current is 15% $f_s = 1.8KHz$, $m = 1$, $V_{DC} = 700V$ and $a = 1.2$. The value of the inductor is calculated and rounded off to 4mH.

4.3.4 Selection of ripple filter:

A high pass first-order filter tuned at half the switching frequency is used to filter out the PCC voltage noise. The time constant of the filter should be very small compared with the fundamental time period T , $R_f C_f \leq T_f$ considering $R_f C_f = T_s/10$ where R_f , C_f and T_s are the ripple filter resistance, ripple filter capacitance, and switching time, respectively. Considering the switching frequency is 1.8KHz, the ripple filter parameters are selected as $R_f = 10\Omega$, $C_f = 5.5\mu F$.

4.3.5 Voltage and Current ratings of IGBTs:

The voltage rating of the device can be calculated by considering a 10% overshoot in the DC link voltage. The voltage rating of the switch is calculated as 440V. With an appropriate safety factor, 600V IGBTs are selected for UPQC VSIs. Considering the ripple current and peak current under dynamic conditions, the current rating is calculated as 50A.

4.4 Fuzzy Logic Controller

The applications of the fuzzy inference method can be found in numerous aspects of industrial production or manufacture. A fuzzy inference system can be an efficient tool to help make decisions on manufacturing reengineering, optimize the process parameters for the drilling process, and realize a better batch process scheduling. All of these applications come with a common point that they are all required to take several factors into account at the same time before reaching a final result. In this kind of problem, the relations between input and output and relations between each input factor are relatively complicated. It is challenging to formulate interactive relations or indirect relations. Therefore, the fuzzy inference system's advantages stand out because the If-Then rule-based inference mechanism can be defined directly by practical experience. Although the most optimal result from accurate mathematical expressions is hard to get, fuzzy inference greatly simplifies and accelerates the computing process and produces a good result for reference [75]. The fuzzy logic process in this study consists of four parts.

4.4.1 Fuzzification Module

The first step is to transform the crisp numerical values of input variables into the appropriate fuzzy sets' equivalent membership values via membership functions. No matter what the input variables describe, through the fuzzification process, the output is usually the degree of membership in the related fuzzy linguistic sets within the interval between 0 and 1. The fuzzification module transforms the system inputs, which are crisp numbers, into fuzzy sets. After identifying the inputs, which are obtained from (12) and (17) in this case, they are split into linguistic variables in the form of simple words. For voltages and currents that are required to be injected, they are labeled as very low, low, average, high, and very high. The corresponding output should also be labeled in terms of linguistic variables, which are nothing but PWM ref voltages in

this project. These are labeled as very small, small, medium, large, and very large. The output values correspond to the duty cycle of the inverters.

4.4.2 Constructing Membership Functions

Numerous literature demonstrates specific applications of fuzzy inference systems in the industry. Still, very little literature introduces a detailed thinking process about setting up appropriate membership functions. It is even more challenging to search available literature discussing membership functions' influence during fuzzy inference. Hashmi (2000) restudied the data selection problem for the drilling process via fuzzy inference. In his Single-Input Single-Output fuzzy inference system, both input and output variables were represented by six identical triangle membership functions. Each of them overlapped the adjacent ones by 50%. Lucian (2006) applied a fuzzy inference system to study the manufacturing reengineering problem. Two or three MFs, respectively, define five input variables. Gaussian MFs, trapezoidal MFs, and general bell MFs with additional support and core are used. This inference system showed a high reliance on professional experience. Srinoi (2008) developed a fuzzy system with four input variables and one output variable for sequencing determination in a flexible manufacturing system [75].

Every input variable was defined by three triangle MFs which overlap with contiguous ones to different extents, while nine triangle MFs subdivided the output variable. Totally 81 ($3*3*3*3 = 81$) kinds of combinations of input variables are expected, and the more finely the output range was divided, the higher the system's resolution could be. And Gheorghe (2013) also used triangle MFs to perform fuzzy inference for specific parts of manufacturing. For all input and output variables, three full-triangle MFs described the middle range of the universe of discourse. Two half-triangle MFs represented the two ends of the discourse domain, respectively. And again, these neighboring MFs overlapped with each other by 50% [75]. After the input and output

variables are fuzzified, they must be defined by a membership function. A membership function (MF) is a curve that represents the feature of a fuzzy set by assigning to each element the corresponding membership value or degree of membership. It maps each point in the input space to a membership value in a closed unit interval $[0, 1]$.

The next step is to quantify the linguistic terms and represent them graphically in a fuzzy set [75]. It maps each fuzzy set to a value in a closed unit interval $[0, 1]$, and it is called membership value or degree of membership. As seen in Figure 7, the x-axis represents an input variable, and the y axis represents the corresponding membership value in the closed interval $[0, 1]$. The number of membership functions (MFs) that are needed to describe the variable, the shape of the MFs, and the overlap ratio with the adjacent MFs, will impact the output. After rigorous analysis in this case, 5 MFs are considered as mentioned before, triangular shape with a 50% overlap ratio with adjacent MFs are chosen.

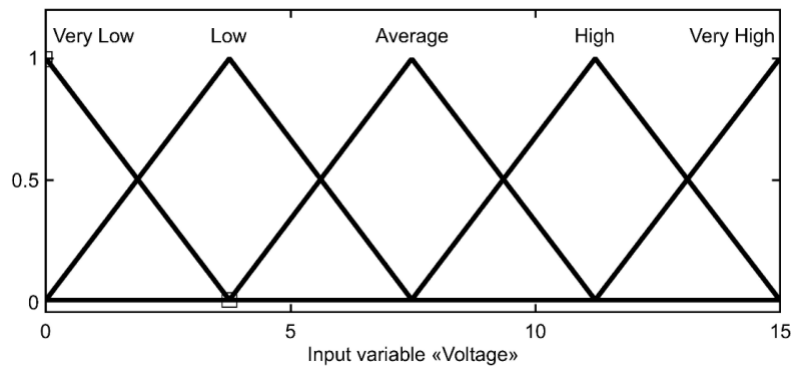


Figure 7. Membership Function for input voltage

Here, the input to 5 level fuzzifier is voltage, and it varies between 0 V and 15 V. Hence, the output, which is a reference voltage to the PWM modulator, also changes, thus varying the duty cycle.

4.4.3 Fuzzy Inference System

Fuzzy inference maps the given input variables to an output space via fuzzy logic-based deducing mechanism, which comprises If-Then rules, membership functions, and fuzzy logical operations. Because the form of the If-Then rule fits in human reasoning, and fuzzy logic approximates people's linguistic habits, this inference process projects crisp quantities onto human language. It promptly yields a precise value as a result, widely adopted [75].

Three types of fuzzy inference methods are proposed in the literature: Mamdani fuzzy inference, Sugeno fuzzy inference, and Tsukamoto fuzzy inference. All of these three methods can be divided into two processes. The first process is fuzzifying the crisp values of input variables into membership values according to appropriate fuzzy sets, and these three methods are precisely the same in this process. Simultaneously, the differences occur in the second process when the results of all rules are integrated into a single precise value for output. In Mamdani inference, the consequent of the If-Then rule is defined by a fuzzy set. A matching number will reshape each rule's fuzzy output set, and defuzzification is required after aggregating all of these reshaped fuzzy sets. But in Sugeno inference, the consequent of the If-Then rule is explained by a polynomial concerning input variables. Thus, the output of each rule is a single number. Then a weighting mechanism is implemented to work out the final crisp output. Although Sugeno inference avoids the complex defuzzification, the work of determining the parameters of polynomials is inefficient and less straightforward than defining the fuzzy output sets for Mamdani inference. Thus, Mamdani inference is more popular, and this thesis only focuses on the Mamdani inference method. Tsukamoto inference seems like a combination of the Mamdani and Sugeno method [75]. The user must create a matrix of rules according to the complexity of the control system. In this control application, the control system involved is a single input single output (SISO) type. So,

there are two fuzzy variables involved in this design. The next step is to form rules according to the system requirements. The fuzzy inference system (FIS) evaluates the rules, and then it combines all of the results to form a final output, which is a fuzzy value, i.e., in the closed interval $[0, 1]$.

4.4.4 Defuzzification

The last step of the fuzzy inference process is defuzzification, through which the combined fuzzy set from the aggregation process will output a single scalar quantity. As the name implies, defuzzification is the opposite operation of fuzzification. Since in the first procedure, the crisp values of input variables are fuzzified into the degree of membership with respect to fuzzy sets, the last method extracts a precise quantity out of the range of fuzzy sets to the output variable. So, this step involves converting output data into a non-fuzzy value, which is a crisp value. This process extracts a scalar quantity as output in the range of the output variable. The output variable's membership function, which is the reference voltage for PWM, is shown in Figure 8. If observed, the square MF shape with a 0% overlap ratio is chosen to get a wide range of outputs. Also, the range of voltages in the x-axis is between 0 V and 1 V, which determines the duty cycle in the PWM modulator circuit. Figure 9 shows the defuzzified output in the form of PWM voltage, which is proceeded to the PWM modulator block, thereby evaluating the modulation index factor. The commonly used Centroid Method [75] has been chosen for this application. It is given by the algebraic expression

$$z_{COA} = \frac{\int \mu_A(z).z dz}{\int \mu_A(z)} \quad (24)$$

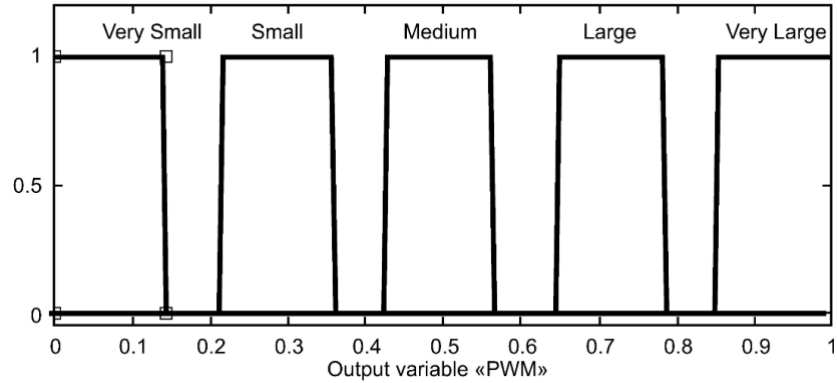


Figure 8. Membership Function for output.

where z is the output variable or PWM reference voltage, and $\mu_A(z)$ is the membership function of the input voltage with respect to output. As shown in Figure 9, the input from the microcontroller is 9.28 V, and the corresponding output from the fuzzy logic controller is 0.618 V.

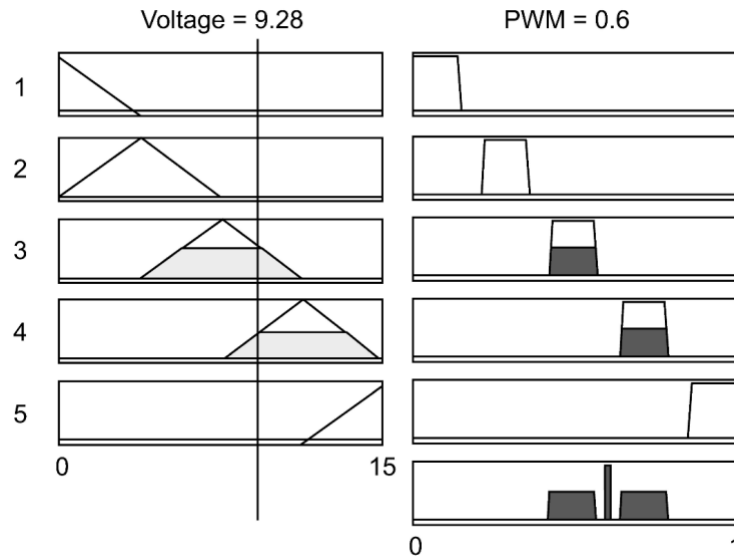


Figure 9. Mapping fuzzy logic inputs and output.

4.4.5 Analysis

The overall process for evaluating the output using a fuzzy logic controller is shown in Figure 10.

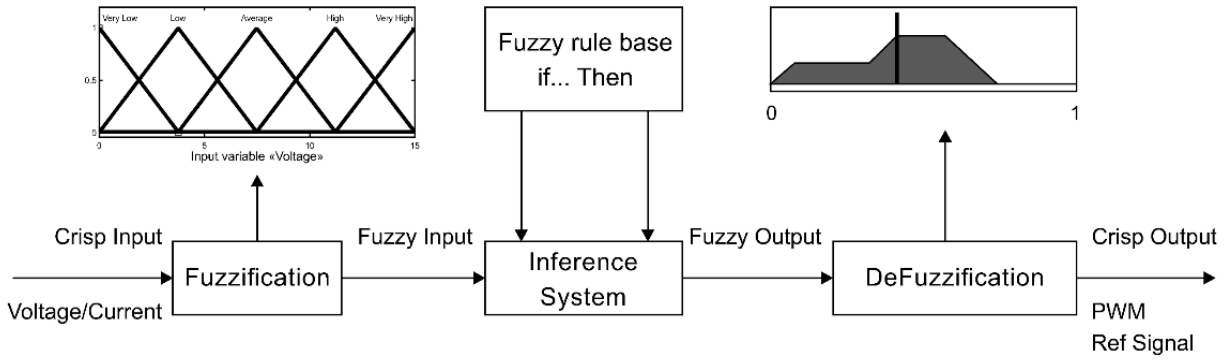


Figure 10. Overview of Fuzzy Logic Controller.

In total, 30 trials were performed to study the effect of overlap ratio among the adjoining MFs. The MFs for the output were separated from the adjacent MFs by a factor of two to acquire the monotonicity of the input-output curve. Then, trials were conducted for selecting the quantity of MF for each variable. Results disclosed that the linearity of the input-output curve is improved when the quantity of the MF increases. The same analogy was applied to evaluate the control design for the shunt inverter. Figure 11 provides the control flow of generating PWM signals using the Fuzzy Inference System. The overall control flow from calculating three-phase reference voltages to generating PWM signals to both the inverters is shown in Figure 11.

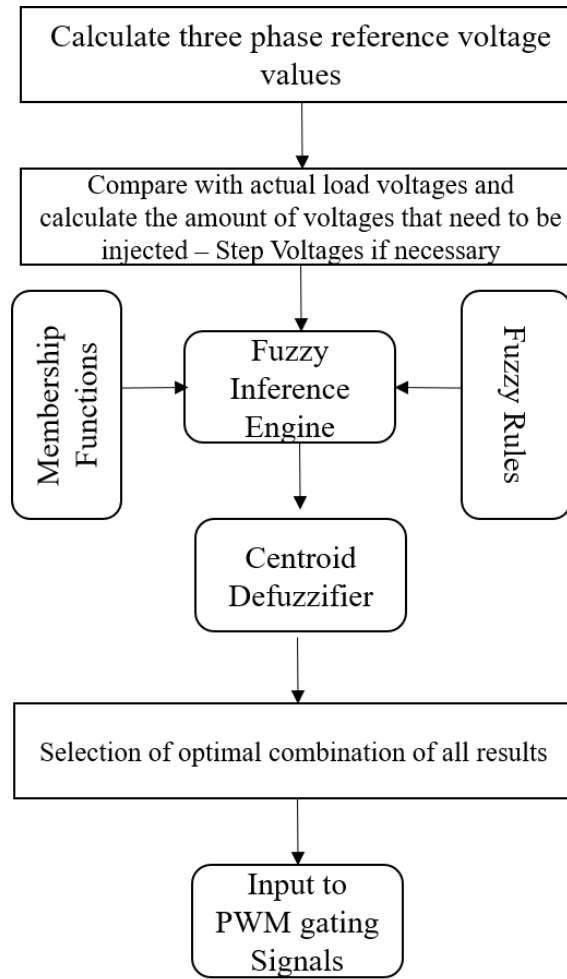


Figure 11. Flow chart of control flow to generate PWM signals.

4.5 Neural Networks

Neural networks, also called artificial neural networks, are an Artificial Intelligence technique that mimics human brain-behavior [74]. Due to its learning and generalization capabilities, neural networks can be expressed as a mathematical representation of the human neural architecture [76]. Neural networks have been used in different areas, such as banking, sales, marketing, education, power, space, etc. They have been applied to medical diagnosis problems, credit ratings, pattern recognition, sales forecasting, and electrical load forecasting. Wherever a relationship exists between explanatory variables (inputs) and explained variables (outputs), neural networks can be applied [74]. They are mostly applicable where the input-output relationship is

complicated or unknown [76]. An artificial neural network includes three layers: input, hidden (invisible), and output. The input layer is expected to receive data from the external environment. The input data may be normalized to improve the results. The hidden layer, which is comprised of neurons, is expected to transform the input into a form that the output can use. The output layer is also comprised of neurons and is expected to produce and present the final outputs. Depending on how the neurons are interconnected, the composition of the layers, and the neurons' disposition, the main architecture of artificial neural networks can be classified as single-layer feedforward neural network, multilayer feedforward network, recurrent network, or mesh network [76]. Multilayer Perceptron (MLP) is one of the main networks using multilayer feedforward architecture. The corresponding feedforward network for this project is, as shown in Figure 12. It consists of an input layer, a hidden layer, and an output layer.

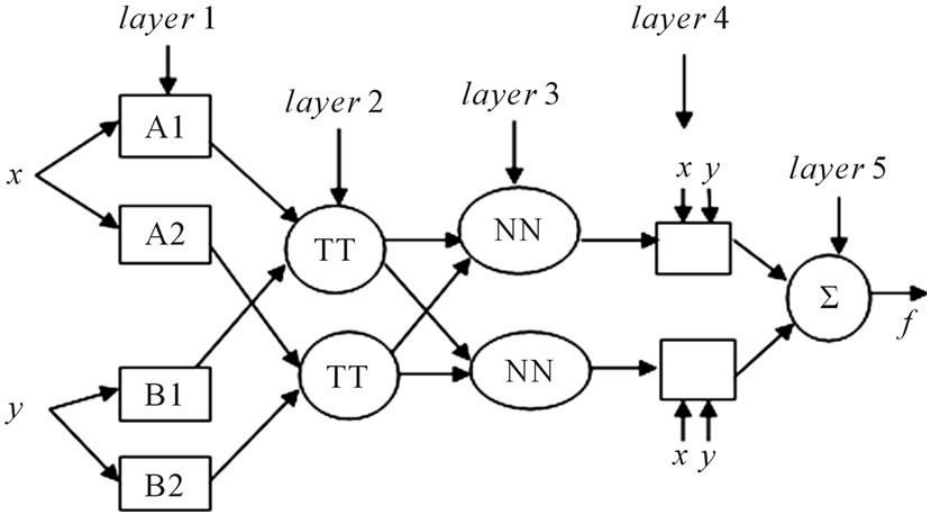


Figure 12. Multilayer Feedforward Network

4.5.1 Algorithm for Neuro Controller:

1. Assume the inputs and outputs in the normalized form with respect to their maximum values, and these are in the range of 0-1.
2. Assure the number of input stages given the network.
3. Indicate the number of hidden layers for the network.
4. Design the new feedforward network based on the system parameters' 'transig' and 'poslin'.
5. Assume the learning rate be 0.02 for the given network.
6. Identify the number of iterations for the system.
7. Enter the goal.
8. Train the network based on the given input and outputs.
9. For the given network, generate simulation with a command 'genism.'

4.5.2 Advantages of Neural Networks:

The advantages of using artificial neural networks are that they are data-driven and do not require any restrictive assumptions on the model's form. They can generalize after training by using the real data the neural network response to the new data that has not been used in the training phase. They can detect complex non-linear relationships between dependent and independent variables. No specific method exists to determine the most appropriate neural network structure before training, so the neural network model is generally designed through a trial and error procedure [76]. In other words, all possible neural network model structures are trained by using the training data set and tested by using the testing data set. The neural network model structure providing the best results, with the smallest error, is eventually selected. Neural network

architectures can be grouped into supervised and unsupervised networks. Supervised neural networks are trained to produce sample inputs. They are well-suited for modeling and controlling dynamic systems and predicting future events. Some of the supervised networks include feedforward, radial basis, and learning vector quantization. Feedforward networks are most commonly used for prediction and pattern recognition and include feedforward backpropagation, cascade feedforward backpropagation, and perception networks. Unsupervised neural networks, such as self-organizing maps, can adjust themselves to new inputs.

For this study, the feedforward backpropagation network was chosen based on the properties of the problem and after experimenting with different network types. Neural networks are retrained until the desired accuracy has been reached. Different training functions exist and are chosen depending on the kind of problem. Scaled Conjugate Gradient and Resilient Backpropagation are appropriate for training large networks and pattern recognition networks [77]. Levenberg-Marquardt is the fastest training function, being suitable for training small- and medium-sized networks. Being one of the most efficient algorithms, Levenberg-Marquardt is highly recommended for neural networks [77]. Considering the features of the problem in this study, Levenberg-Marquardt was chosen as the training function. And Figure 13 shows the mapping of input and output layers designed in MATLAB for this project.

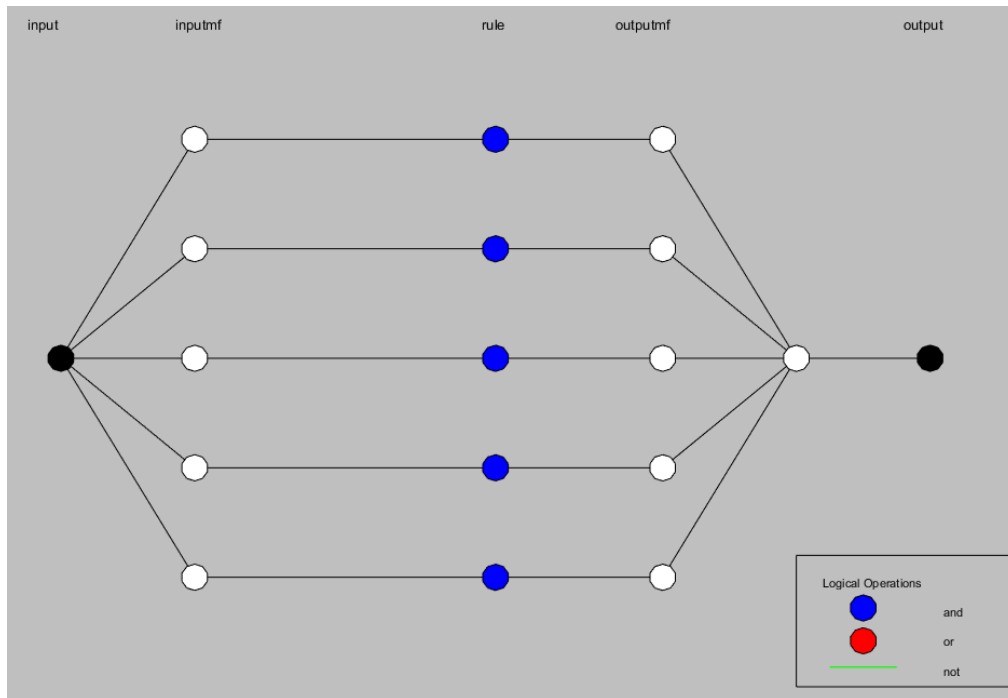


Figure 13. Mapping ANFIS inputs and output

4.6 ANFIS Acclimation

An adaptive neuro-fuzzy inference system (ANFIS) is based on the Sugeno fuzzy inference system. It consolidates both the fuzzy logic and neural network laws, and this integrated system has the potential to capture the benefits of both of the systems in a single framework. The membership functions' behavior depends on specific parameters, and any variation in the parameters will alter the behavior of the membership function. Instead of arbitrarily choosing the membership function parameters based on user analysis, the ANFIS structure determines membership function parameters automatically. ANFIS was introduced by Jang [78]. ANFIS is used for modeling, controlling, and parameter estimation in complex systems. ANFIS is a combination of an artificial neural network (ANN) and fuzzy inference system (FIS). Combining the ANN and fuzzy-set theory can provide advantages and overcome the disadvantages in both techniques.

The ANFIS model can be trained without relying solely on expert knowledge sufficient for a fuzzy logic model. The ANFIS model has the advantage of having both numerical and linguistic knowledge. ANFIS also uses the ANN's ability to classify data and identify patterns. Compared to the ANN, the ANFIS model is more transparent to the user and causes fewer memorization errors. Consequently, several advantages of the ANFIS exist, including its adaptation capability, non-linear ability, and rapid learning capacity. This approach is essentially a rule-based fuzzy logic model whose rules are developed during the model's training process. The training process is data-based. ANFIS constructs a fuzzy inference system (FIS) whose membership function parameters are derived from the training examples. The most commonly used fuzzy inference systems are Mamdani and Sugeno. Mamdani and Sugeno's main difference is that the Sugeno system's output membership functions are either linear or constant [78]. However, the output membership functions of the Mamdani system can be triangular, Gaussian, etc. In this study, the Sugeno-type fuzzy inference system was used because the Sugeno-type system is more computationally efficient than the Mamdani type. The Mamdani type is more reliant on expert knowledge. However, the Sugeno type is trained by real data [79].

4.6.1 Creating a Sugeno System

So far, Mamdani systems have been used, but ANFIS supports only the Sugeno type system. This is no different than the previously created one, except there is no defuzzification method to evaluate as it is accounted for by the ANFIS system.

4.6.2 Know your Data

As the emphasis is on the real-time data, training data has to be tabulated. The parameters are associated with membership functions and change accordingly during the learning process. These parameters are assisted by a gradient vector, which provides a measure of input-output data

for a given set. The ANFIS in this current project uses a backpropagation algorithm for membership function parameter estimation [80]–[82].

4.6.3 Implementation

Before hardware implementation, MATLAB provides several options for evaluating the data that needs to be used in training the ANFIS controller. Different layers are involved in the ANFIS controller; however, this study has not been emphasized as many research articles have provided explanations for this process [83]. Figure 14 shows the PWM output from the given set of training data to the ANFIS controller. The PWM output voltage then calculates the modulation index, thereby deciding the percentage of duty cycle to be fed to the inverter. The overall process for the ANFIS controller is shown in Figure 14.5.

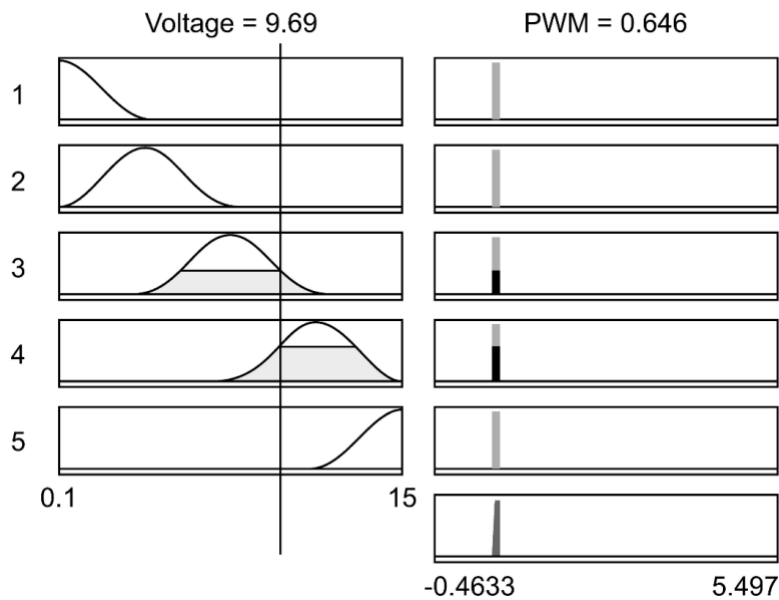


Figure 14. Mapping ANFIS inputs and output

Figure 15 gives the output captured from the ANFIS controller, which will be the input for the PWM modulator circuit, as shown in Figure 3. The three reference sinusoids are 120° apart to produce a balanced three-phase output.

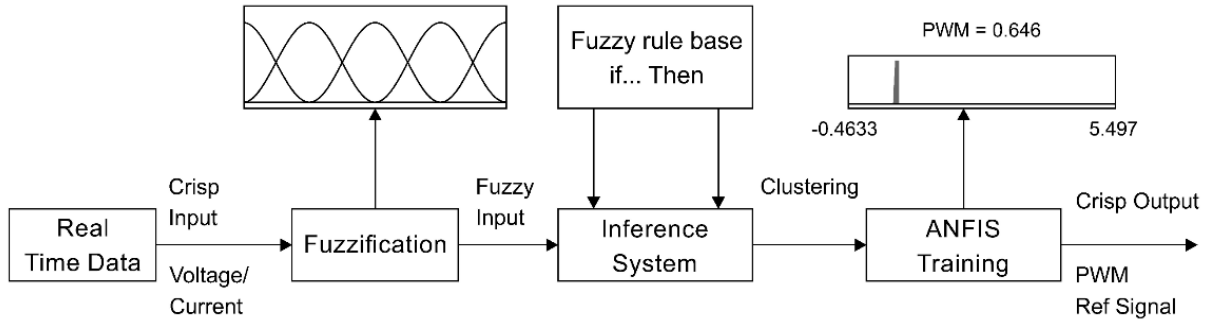


Figure 15. Overview of ANFIS Controller.

Figure 16 shows a triangular carrier and the three-phase reference waves, which are the ANFIS/fuzzy logic controller outputs. The switching pattern for the six IGBTs in view of the series inverter and the shunt inverter are shown in Table 1 determines the ON-OFF conditions for both of the inverters in accordance with the output obtained from the controller. Harmonics will be minimized if the carrier frequency is chosen to be an odd triple multiple reference frequency. Figure 16 shows output waveforms for voltage from the inverter between phase to neutral and phase to phase.

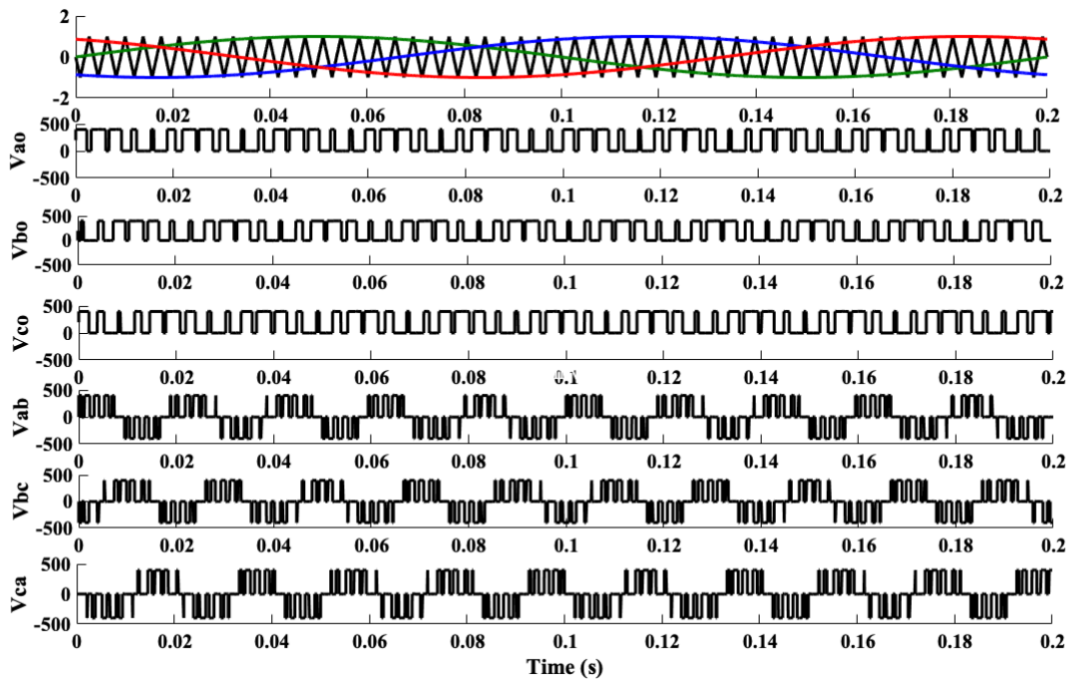


Figure 16. Waveforms of three-phase inverter corresponding to the PWM signal.

Table 1 Switching Pattern for Series and Shunt Inverters

Case	Series Inverter	Shunt Inverter
$V_a > V_{tri}$	Q1 ON	Q7 ON
$V_a < V_{tri}$	Q2 ON	Q8 ON
$V_b > V_{tri}$	Q3 ON	Q9 ON
$V_b < V_{tri}$	Q4 ON	Q10 ON
$V_c < V_{tri}$	Q5 ON	Q11 ON
$V_c > V_{tri}$	Q6 ON	Q12 ON

A commercially available microcontroller (MSP430x14x) was used in this application to implement the ANFIS controller. The block diagram for implementing the system in real-time is shown in Figure 17. The microcontroller is sourced by a 5 MHz high-resolution clock that is used for PWM generation. After setting up the clock system, the peripherals were configured. The MSP430 watchdog timer was set as an interval timer. The Interrupt Service Routine (ISR) function was programmed to wake up the CPU from low-power mode.

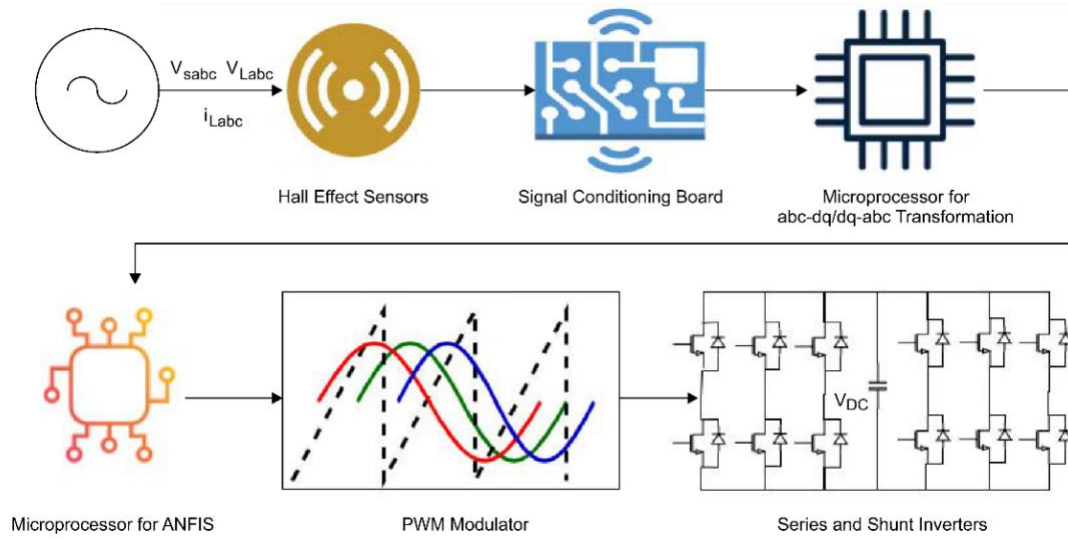


Figure 17. Real-time implementation of the ANFIS control system.

After peripheral configuration, the actual control loop was entered, and the input 'voltage' is calculated based on training data using the ANFIS mechanism.

system is simulated under different conditions; a secondary distribution system model analogous to the IEEE 30 bus system was designed [84]-[86]. The system was designed to connect primary feeders and lateral feeders to the secondary feeders. It was then modeled from the substation transformer, as shown in Figure 18 to the household level. Each feeder was connected to an individual type of linear and/or non-linear load and only some are shown for simplicity. The data for this case study is taken from [87]–[90]. Several scenarios were tested, and the key results are presented in this section.

5.1 Voltage and Power magnitudes

The UPQC for this 30-feeder distribution system was designed according to its suitable voltage levels, is also built for a secondary distribution level. The proposed UPQC-P was applied at PCC, and faults were applied at three different locations: viz., feeder 4, feeder 12, and feeder 14 of the test system. The active and reactive power flows along with the voltages were studied at these buses with and without the application of UPQC-P under a fault condition. The fluctuations in the amplitude of voltage in relation to the variations of active and reactive power flows were studied carefully during fault conditions.

5.1.1 Three-Phase-to-Ground Fault (LLL):

A 10 kVA UPQC is connected to feeder 4 to assess its contribution to the restoration of network voltages during the sag. Initially, three-phase faults are simulated in the network without the UPQC, and voltages at all other network feeders are calculated. Faulted feeders are selected so that the faults resulting in voltage sags at feeder 4 have magnitudes ranging from 0.1 p.u. to 0.9 p.u. Sag calculation is then repeated with the UPQC connected at feeder 4. The resulting network sag performance is illustrated in Figure 19 and 20. It can be seen that UPQC improves voltages for all faults, mainly those that are electrically close to feeder 4. The bus voltage is plotted on the Z-

axis, and active-reactive powers are plotted on the X and Y axes, respectively. The bus voltage's overall improvement is about 30%, which is proportional to the sag amount.

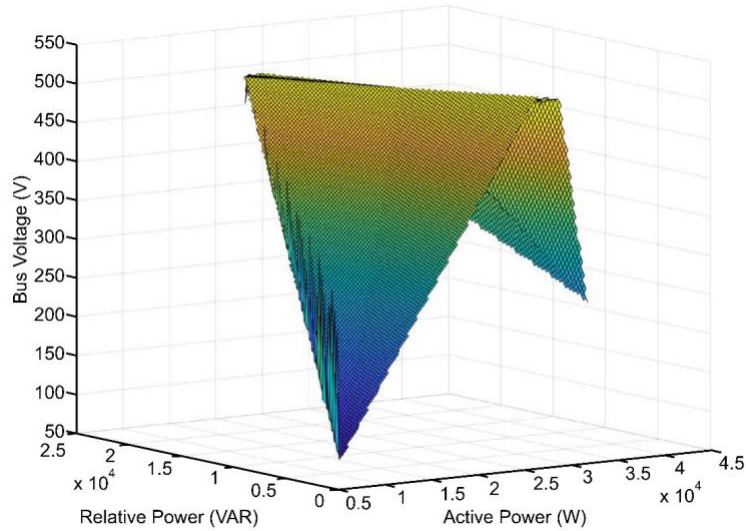


Figure 19. Sag magnitudes with a three-phase fault at feeder 4.

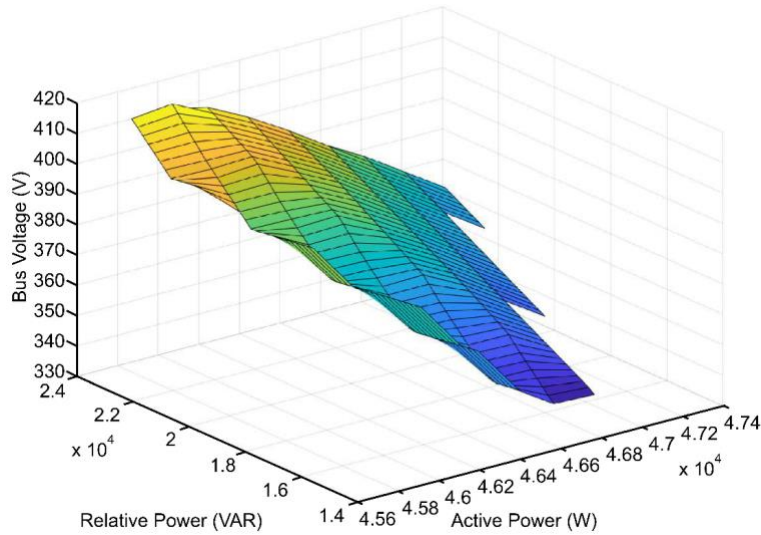


Figure 20. Reduced sag magnitudes with the application of the UPQC at feeder 4.

5.1.2 Single-Phase-to-Ground Fault (LG):

LG faults (phase A is the faulted phase) are simulated at feeder 12, and the results of the calculation illustrated in Figure 21 and 22. It can be seen that the UPQC compensates voltage magnitudes in all three phases. It injects reactive power when the sag voltage is below the pre-

fault value and absorbs reactive power when the swell voltage is above 1.1 p.u. Voltages in feeder 12 are either brought within the 10% limit or smoothened.

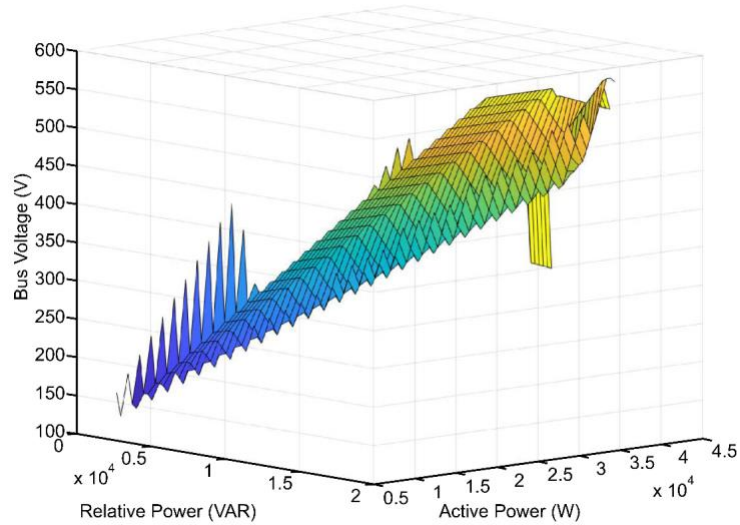


Figure 21. Voltage and power magnitudes during a fault condition at feeder 12.

On comparing Figure 21 and 22, it can be seen that the UPQC with the proposed ANFIS controller improves voltage magnitudes and reduces the rapid distortions in power. Power and voltage distortions were compensated within a time frame of 0.3 s, which indicates the controller response time.

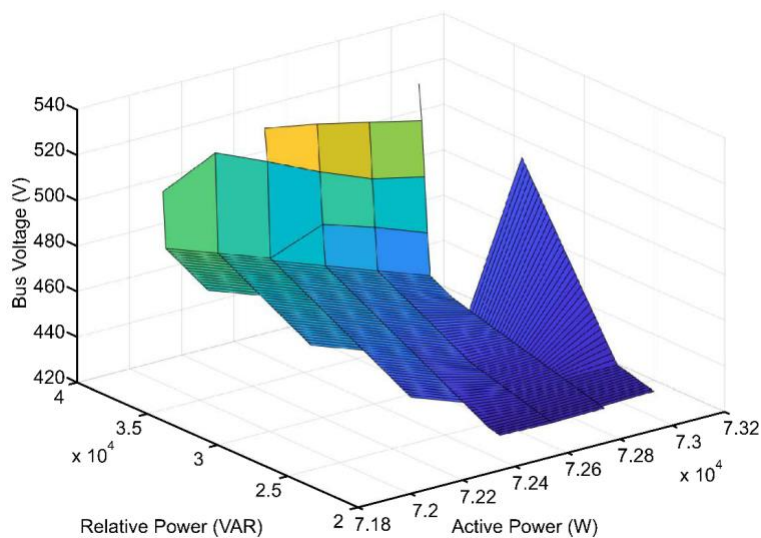


Figure 22. Effect of ANFIS UPQC-P connected at feeder 12 after the fault.

5.1.3 Double-Phase-to-Ground Fault (LLG):

LLG faults phase A and B are the faulted phases are simulated at feeder 14, and the results were shown in Figure 23 and 24. It can be seen that with a UPQC connected at feeder 14, the voltage magnitudes are all improved by mitigating the voltage sags.

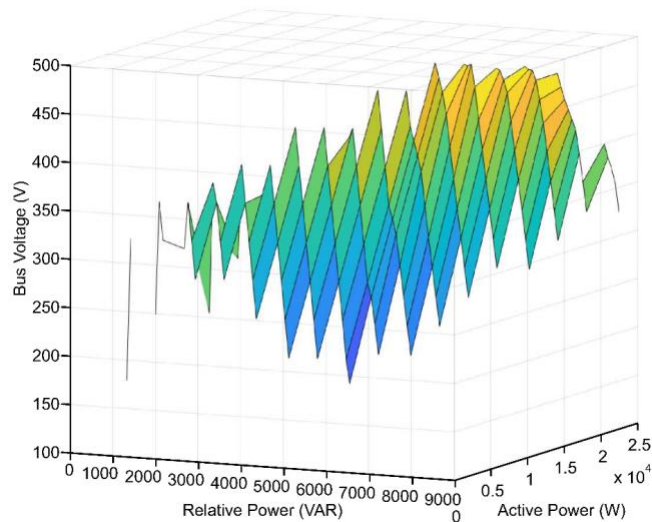


Figure 23. Line to line fault at feeder 14.

The effect of the UPQC is pronounced clearly in Figure 24. The dip in power in Figure 23 occurred during the fault condition; during this time frame, the ANFIS control algorithm calculated the error signal and produced proper gating signals for both the inverters to input the required voltage and current. As in all previous cases, voltages in all phases were significantly improved by UPQC. The amount of restoration depends on the severity of the fault and the P, Q capability of the UPQC.

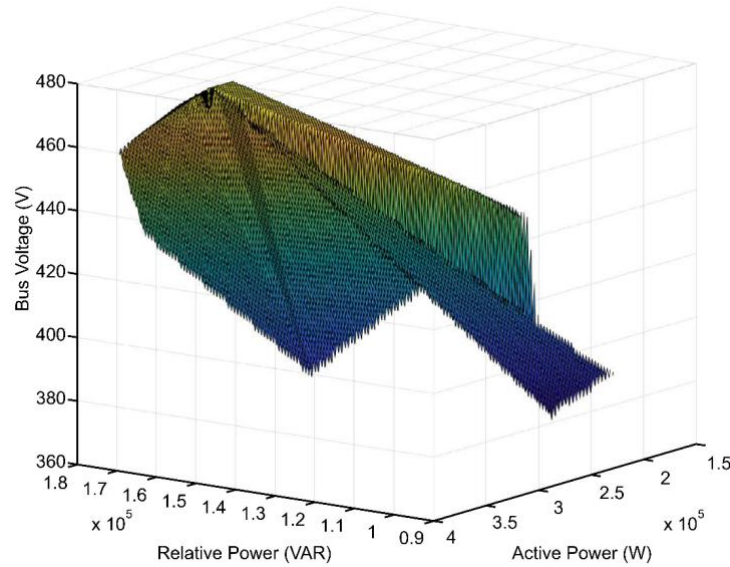


Figure 24. Reduced spikes in voltage under UPQC-P at feeder 14.

5.2 Voltage and Current waveforms

This section deals with the fundamental voltage and current waveforms of the interconnected system, which interprets a) the distorted voltage waveforms of the main grid as the voltage disturbances result from the source side, and the distorted current waveforms of microgrid are due to the presence of non-linear loads, b) the necessary injection of both voltage and currents by the UPQC, which shows its effect, and c) the desired microgrid voltages and harmonic-free main grid currents. The three-phase source voltages are demonstrated in Figure 25, which shows the system grid voltages under the fault condition. The fault condition is created in the distribution side before the point of common coupling. The type of fault created is temporary. The UPQC-P responds to this voltage sag condition within minimum time, and DVR acts by injecting the necessary voltage, as shown in Figure 26 and 27 shows the voltages at PCC returning to normal voltage levels.

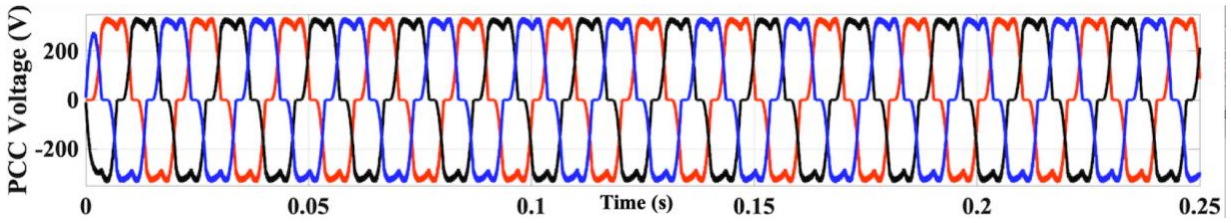


Figure 25. PCC voltage under fault condition.

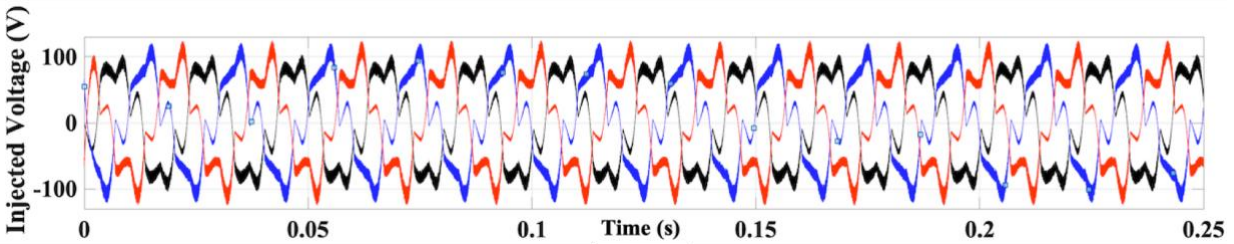


Figure 26. Injected voltage by the DVR.

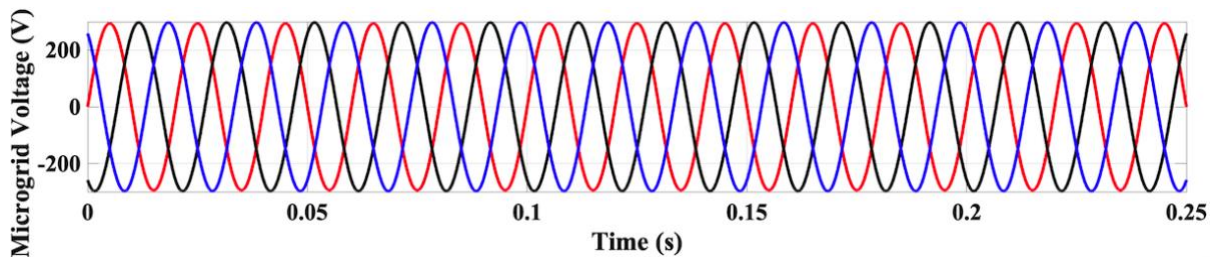


Figure 27. Pollutant free voltages at PCC.

Similarly, Figure 28 demonstrates the results of load currents on the consumer end. Under a fault condition, the DSTATCOM of the UPQC-P acts on reducing the harmonic content. Due to the occurrence of the temporary three-phase fault (self-clearing fault) before the point of common coupling, the system experiences voltage interruption in the short period. Figure 28 shows the distorted currents, Figure 29 shows the effect of the proposed controller, and Figure 30 gives the harmonic-free content in the grid.

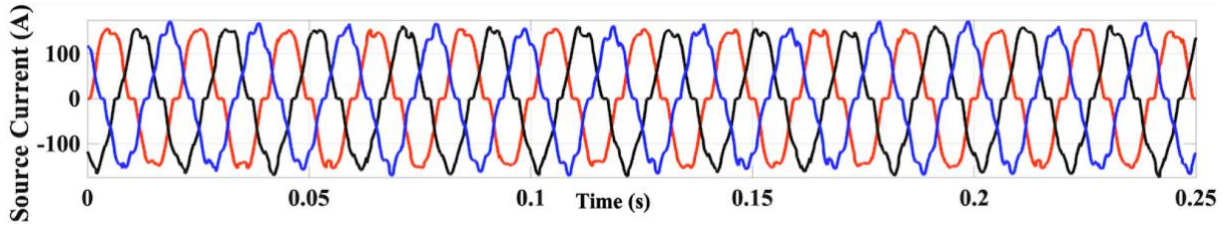


Figure 28. Harmonic content in source currents.

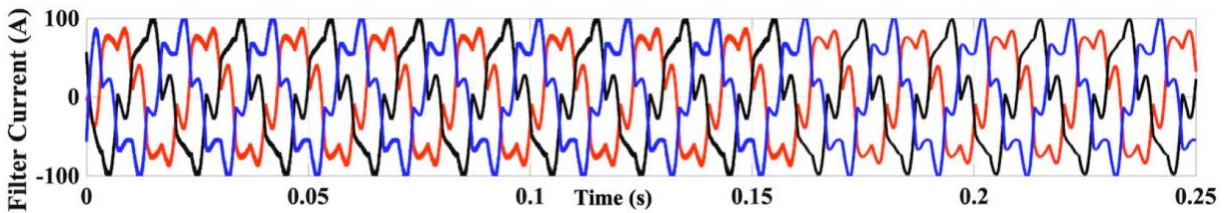


Figure 29. Injected current by the DSTATCOM.

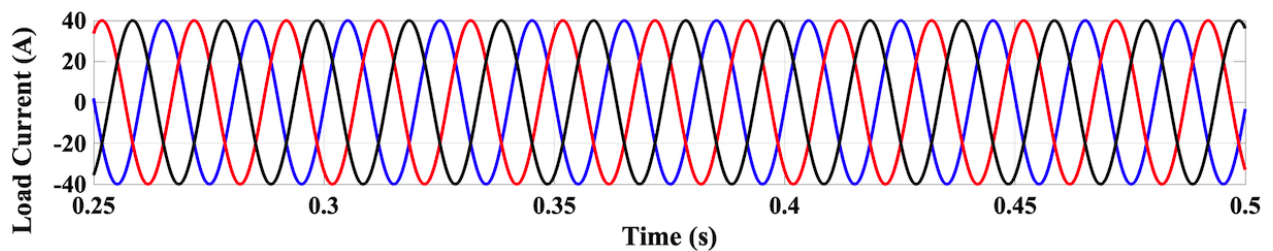


Figure 30. Pollutant free currents at the consumer load end.

5.3 FFT Analysis

This segment deals with the Fast Fourier Transform (FFT) analysis in which the total harmonic distortion (THD) content of the system is extracted from the simulated interconnected system. The FFT is a mathematical technique for transforming a function of time into a function of frequency. In some cases, it is depicted as transforming from the time domain to the frequency domain. It is beneficial for the analysis of time-dependent phenomena. Comparison of THD content of load currents with different controllers are made in the following section, which displays noticeable changes after employing converters starting with PI, then fuzzy logic, and finally, by employing the ANFIS-based controller. As per IEEE 519 standards, for systems 69 kV and below, the harmonic distortion factor is limited to 5% [91].

5.3.1 Case 1: Without any Controller

The proposed system was tested under no controller operation to demonstrate the impacts of various controllers starting with Figure 31.

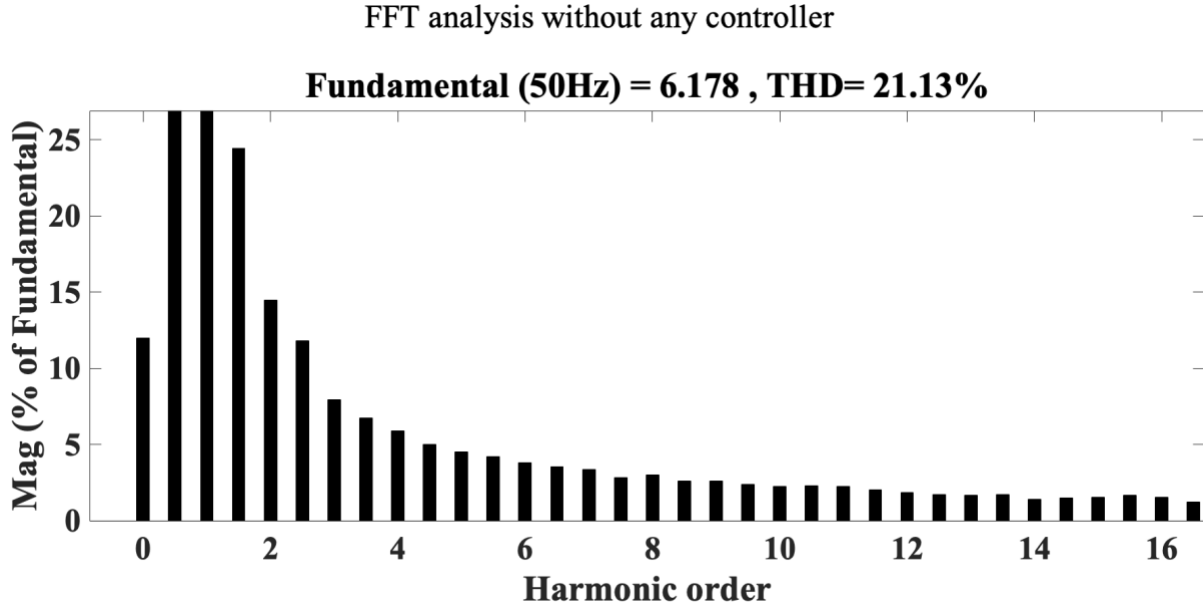


Figure 31. THD of load currents without any controller.

5.3.2 Case 1: With PI Controller

The proposed system was tested with the simple PI technique to control both VSIs and decrease the distortion content. The traditional PI controller is straightforward in nature and operates on gain factor. It reduced harmonics to some extent, with a THD content of 14.74%, as shown in Figure 32.

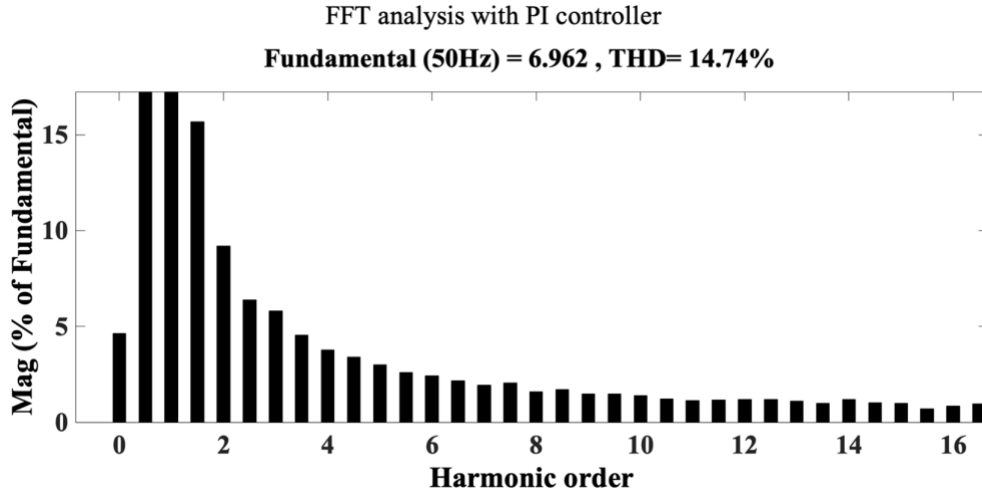


Figure 32. THD of load currents with PI controller.

5.3.3 Case 2: With fuzzy controller

Using the fuzzy controller, the harmonics were further reduced, to a THD content of 6.13% as shown in Figure 33.

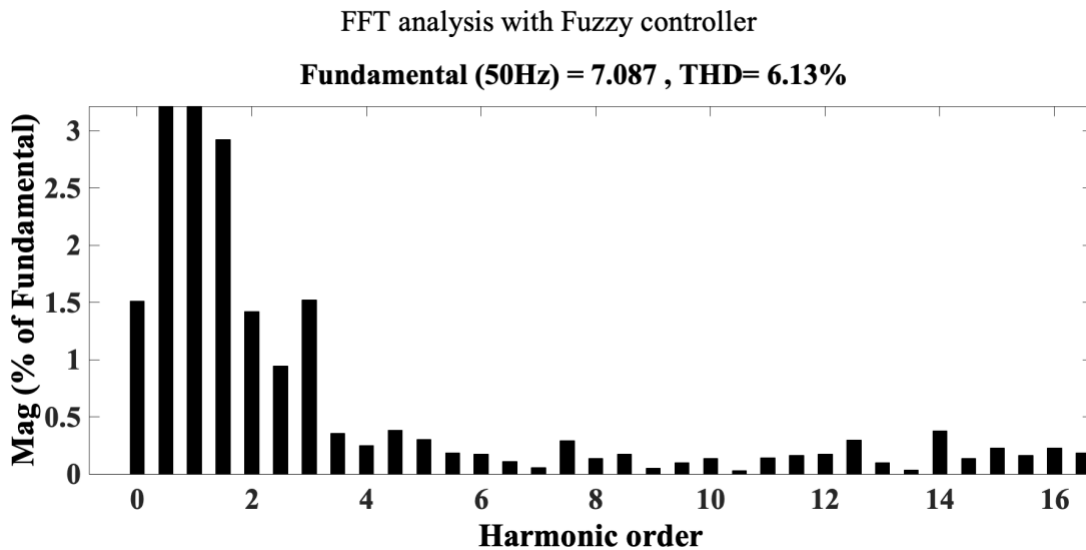


Figure 33. THD of load currents with Fuzzy controller.

5.3.4 Case 3: With ANFIS controller

As seen above, both PI and fuzzy controllers successfully reduced the THD to some extent, but it can be filtered further using the ANFIS controller, as shown in Figure 34. In this case, the

THD content has decreased to a value of 2.43%, which is well within IEEE 519 standards' recommended limits.

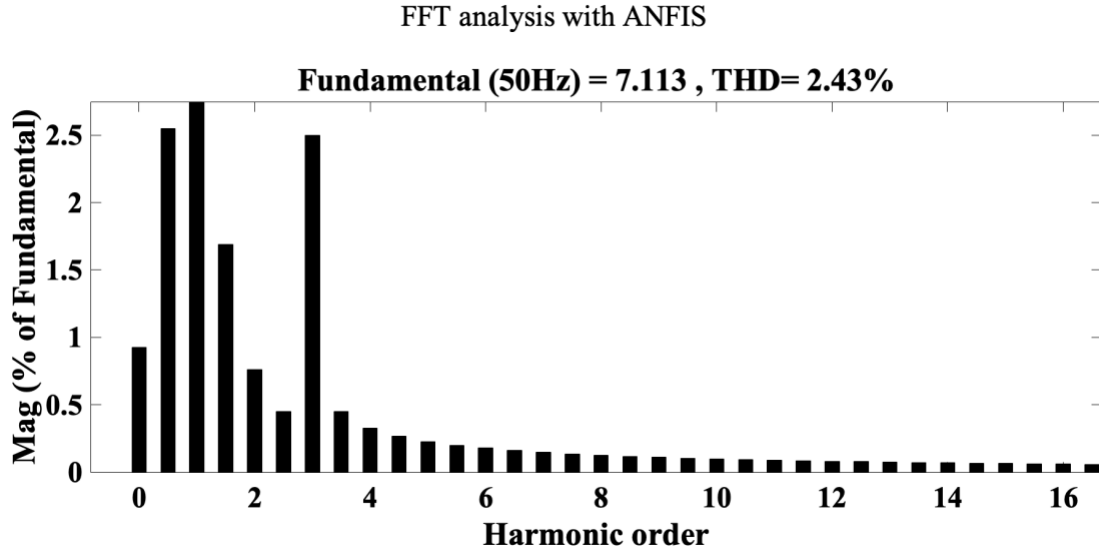


Figure 34. THD of load currents with ANFIS controller.

5.4 Experimental Validation

To validate the operation of the proposed scheme, a UPQC prototype topology with shunt and series converter rating 1 kVA, as shown in Figure 4 is developed. The control system for the UPQC-P is developed per Figure 17. The UPQC is realized with two Metal Oxide Semiconductor Field Effect Transistor (MOSFET) modules.

5.4.1 Schematic Design

The schematic of the proposed UPQC, including the inverters, control circuit boards were designed using Autodesk Eagle software, as shown in Figure 35. Generating PWM signals to both the inverters using a fuzzy logic controller through microprocessors is crucial in this design. Several op-amps, a driver circuit, microprocessors were involved in this design, and only the driver circuit is shown in the schematic.

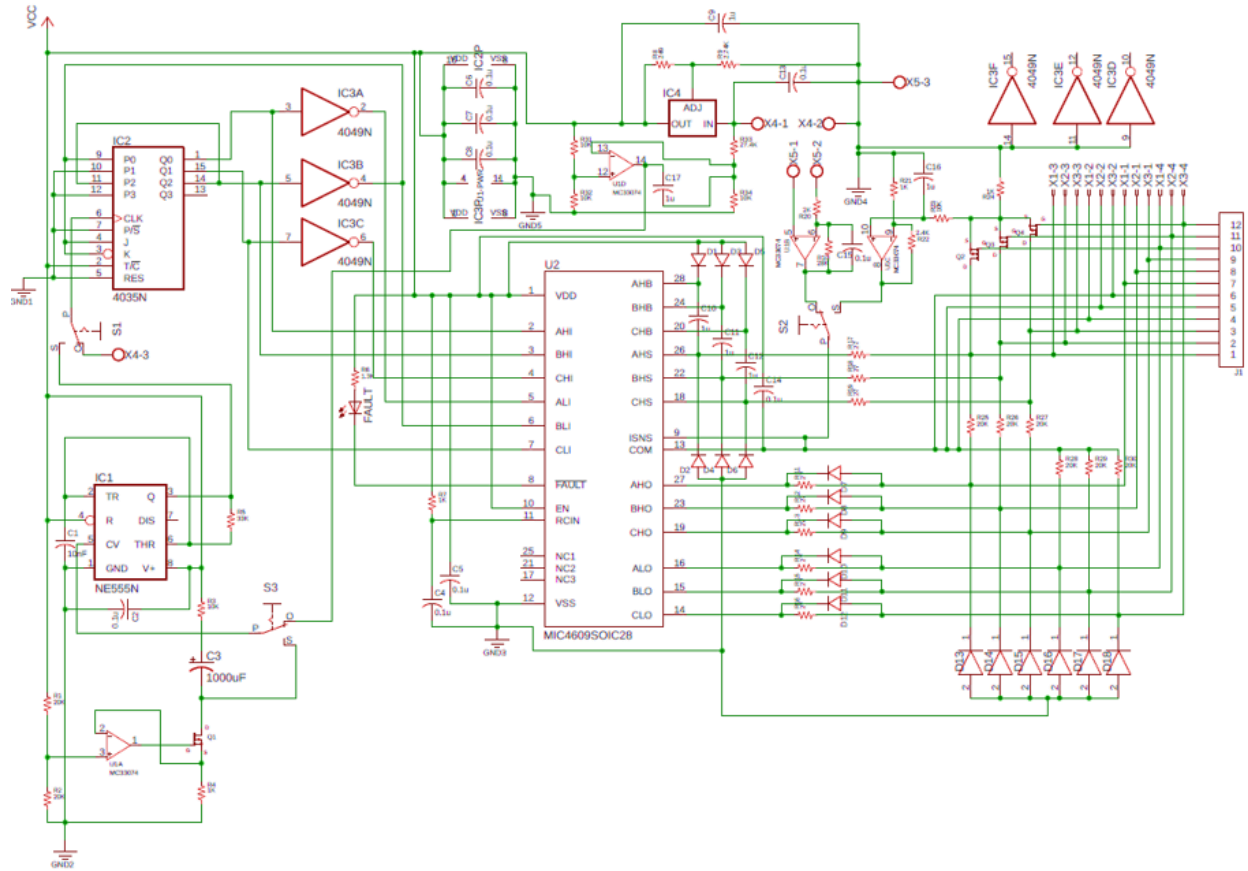


Figure 35. Control diagram schematic for VSIs.

5.4.2 Prototype Design

The prototype design represents the complete assembly of the overall system of the UPQC, including series VSI, shunt VSI, DC link capacitors, signal conditioning boards, and load. The complete experimental setup is shown in Figure 36.

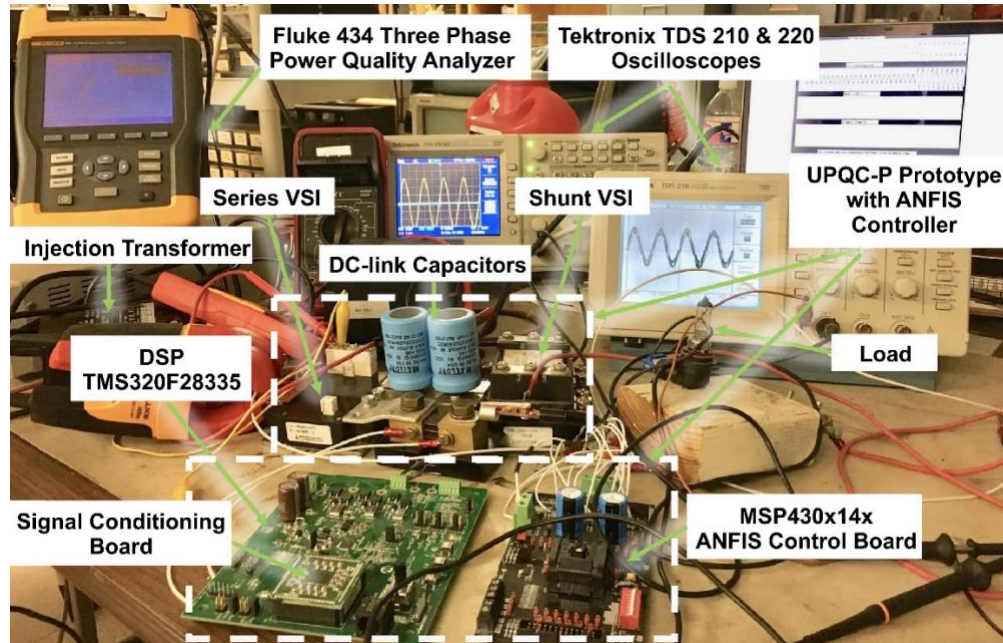


Figure 36. Experimental setup with the prototype UPQC-P.

5.4.3 Experimental Results

The experimental results are presented in Figures 37-39. These results are for the prototype shown in Figure 36 that was tested under a 1 kW load condition for different voltage sag and swell operating conditions. The results are configured by designing a proper shunt, through which the voltages are calculated and scaled to source and load current values. In Figure 37, the grid voltage was shown distorted under a fault condition. The grid voltage is around 180V under this sag condition. DVR injects the necessary voltages into the grid, as shown in Figure 38. And the load voltages are restored to a normal level, as shown in Figure 39.

Similarly, the current waveforms from the experimental setup can be observed from Figures 40-42. The harmonics in the source currents due to a faulted condition in response to Figure 37 is shown in Figure 40. The DSTATCOM part of the UPQC has compensated currents to reduce harmonic content shown in Figure 41. As a result, clean load end currents are obtained in Figure 42.

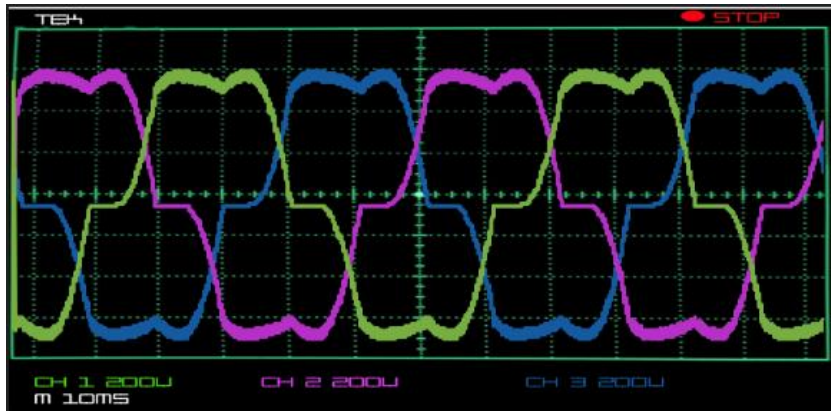


Figure 37. Grid voltage under fault condition.

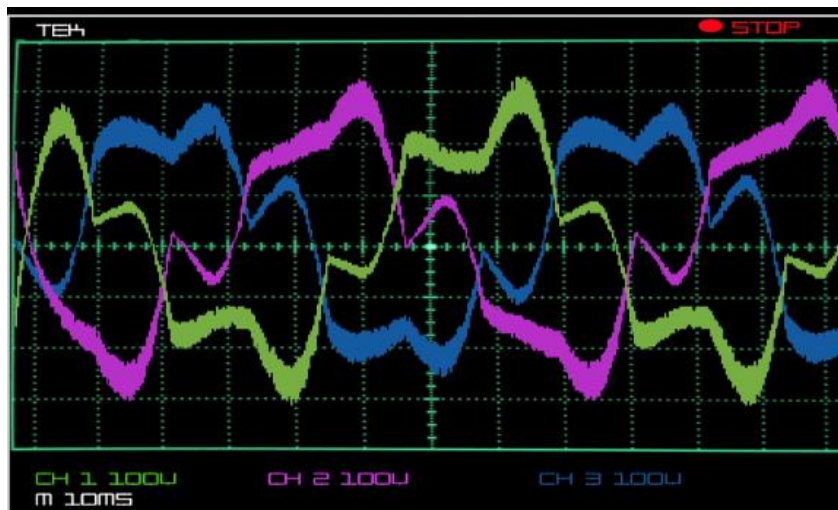


Figure 38. Injected voltage by the UPQC.

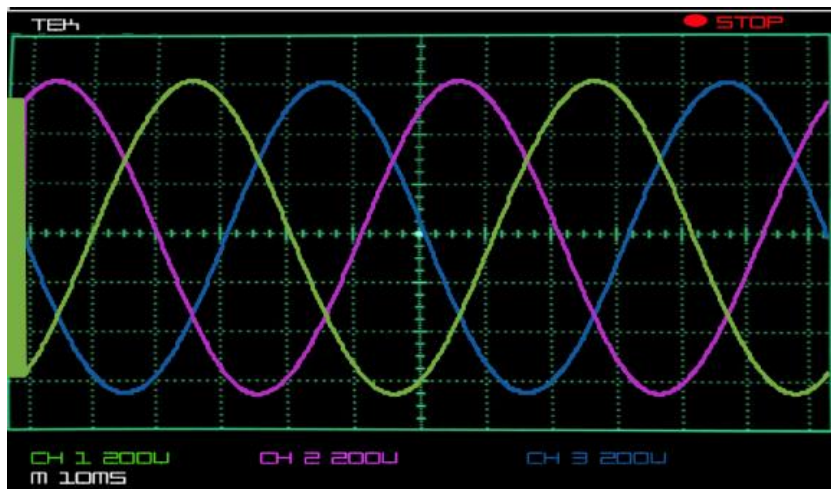


Figure 39. Pure voltages at PCC.

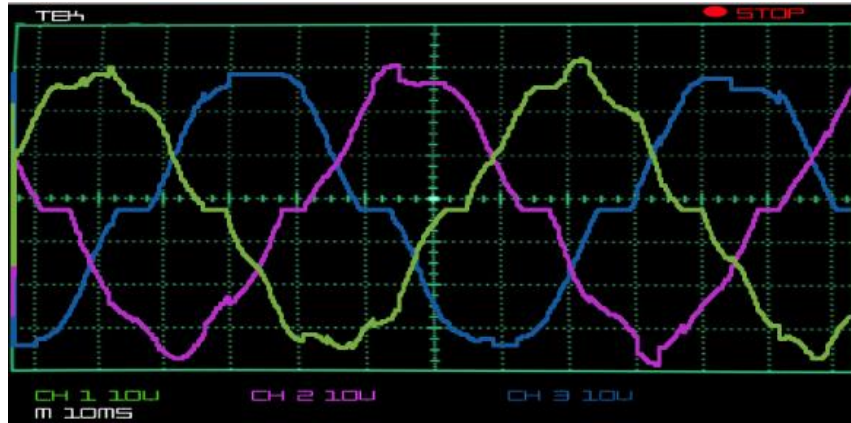


Figure 40. Harmonics in source currents.

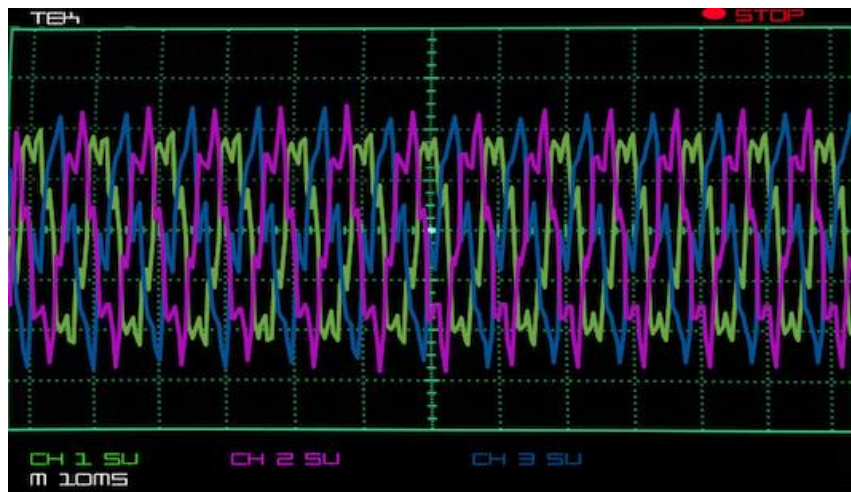


Figure 41. Injected current by UPQC.

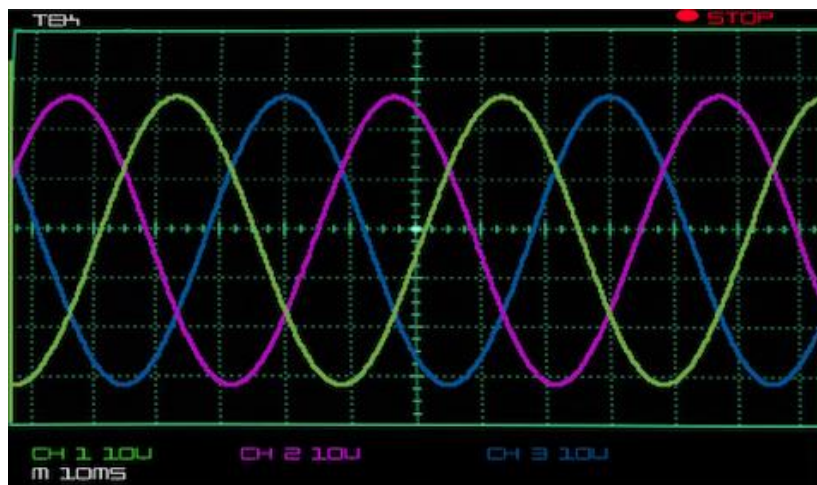


Figure 42. Clean load end currents.

The design parameters are taken, as shown in Table 2. The simulation results and the experimental results are very close and demonstrate the proposed controller performance under pragmatic conditions.

Table 2 UPQC Prototype Parameters

Parameter	Value
Voltage	230 V
Grid frequency	60 Hz
Power rating	1 kVA
DC-link voltage	300 V
DC-link capacitors	10 μ F
Series and Shunt VSI Filters	$L_f = 0.8$ mH; $R_f = 2$ Ω ; $C_f = 0.5$ μ F
Switching frequency	1.8 kHz
Voltage rating of IGBTs	400 V
Current rating of IGBTs	2 A

CHAPTER 6

CONCLUSIONS

With the increased capability of different kinds of renewable energy resources at the standard household level and integrating the microgrid and main grid, the lack of state-of-the-art methods for ensuring consistent power quality is a major challenge. To regulate voltage and ensure harmonic and distortion-free currents at the consumer end, an advanced control system using a UPQC-P is proposed. Comparison with different control techniques were presented in Figure 43.

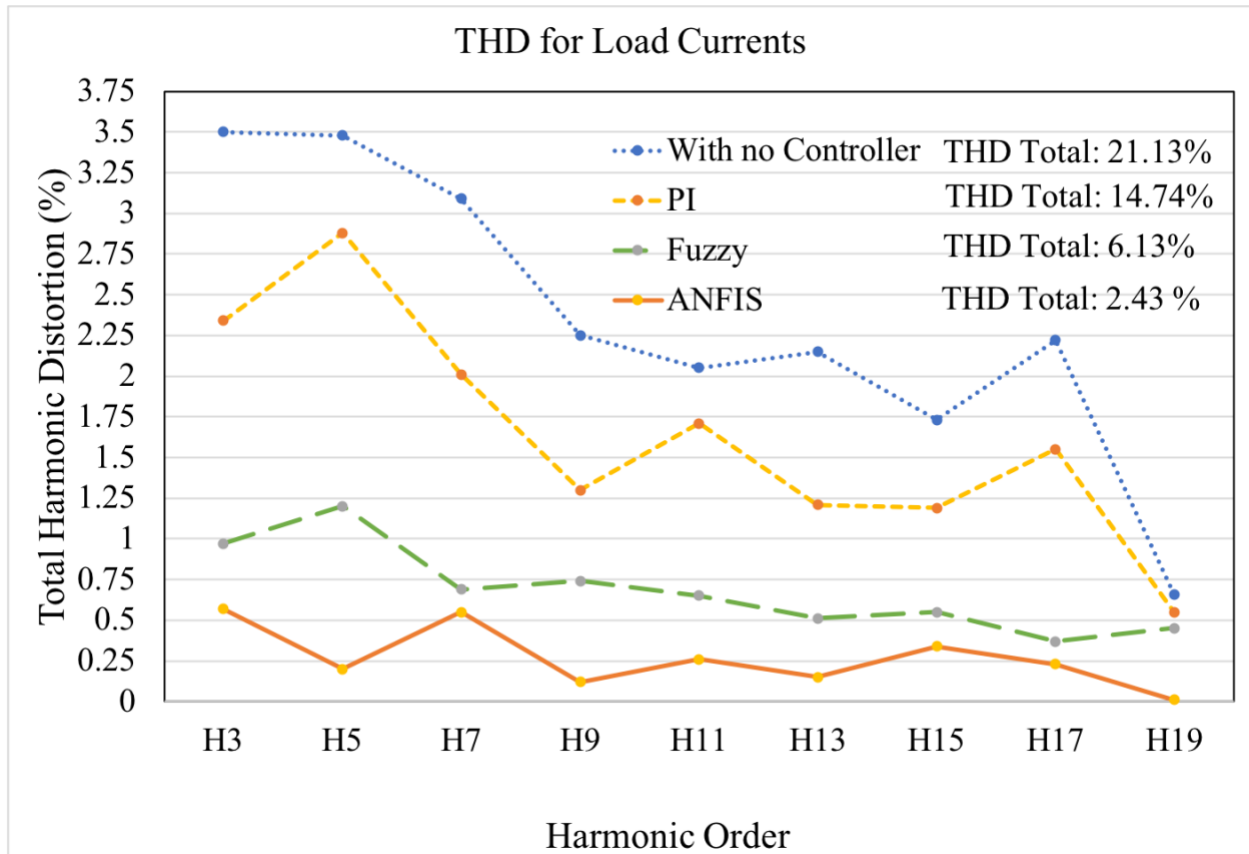


Figure 43. THD comparison for load currents with different controllers.

The device is installed at PCC with the microgrid and other electrical loads connected to and designed to deal a wide range of PQ problems. The design concept has been tested under several conditions, and results shown the unique, controlling action handling variety PQ issues,

thus increasing overall reliability at PCC. The proposed system was evaluated using MATLAB/Simulink. Furthermore, a prototype of the model, named UPQC-P, was developed. It was applied to a 30-feeder distribution system having several types of faults, and the voltage and power magnitudes at several buses were closely monitored. The proposed control strategy responded within a timeframe of 0.3 s, reduced peak voltage distortions, and restored voltage to a normal level at the interconnecting point. Moreover, the THD content of currents decreased from 21.13% to 14.74% when a PI technique was used to control the UPQC-P. Finally, in this scenario, the proposed ANFIS-based UPQC-P was able to reduce the harmonic content to 2.43% from 21.13%.

REFERENCES

REFERENCES

- [1] Marnay, C., Bailey, O.C.: The CERTS microgrid and the future of the macrogrid. Lawrence Berkeley National Laboratory. Lawrence Berkeley National Laboratory: Lawrence Berkeley National Laboratory. Retrieved from: <http://escholarship.org/uc/item/1103m944>
- [2] Wang, F., Duarte, J.L. Hendrix, M.A.M.: 'Grid-interfacing converter systems with enhanced voltage quality for microgrid application—concept and implementation', IEEE T. Power Electr., 2011, 26, (12), pp. 3501–3513
- [3] Basso, T.S: 'System Impacts from Interconnection of Distributed Resources: Current Status and Identification of Needs for Further Development', Technical Report NREL/TP-550-44727 January 2009
- [4] Liu, Zhanhe, "Power Quality Study of a Microgrid with Nonlinear Composite Load and PV Integration" (2015). All Theses. 2459. https://tigerprints.clemson.edu/all_theses/2459
- [5] G. Venkataramanan and C. Marnay, "A larger role for microgrids," Power and Energy Magazine, IEEE, vol. 6, pp. 78-82, 2008
- [6] Hingorani, N.G.; Gyugyi, L. Understanding FACTS: Concepts and technology of Flexible AC Transmission Systems; IEEE Press: Piscataway, NJ, USA, 2000; pp. 1–35.
- [7] Georgilakis, P.S.; Hatziargyriou, N.D. Unified power flow controllers in smart power systems: models, methods, and future research. IET Smart Grid 2019, 2, 2–10
- [8] Meikandasivam, S.; Nema, R.K.; Jain, S.K. Fine power flow control by split TCSC. Int. J. Electr. Power Energy Syst. 2013, 45, 519–529
- [9] Johansson, N.; Angquist, L.; Nee, H.P. An adaptive controller for power system stability improvement and power flow control by means of a thyristor switched series capacitor (TSSC). IEEE Trans. Power Syst. 2010, 25, 381–391
- [10] Wang, L.; Vo, Q.S. Power flow control and stability improvement of connecting an offshore wind farm to a one-machine infinite-bus system using a static synchronous series compensator. IEEE Trans. Sustain. Energy 2013, 4, 358–369.
- [11] Liu, J.; Xu, Z.; Fei, W.; Chen, L.; Chen, B.; Chen, B. Comprehensive power flow analyses and novel feedforward coordination control strategy for MMC-based UPFC. Energies 2019, 12, 824.
- [12] Yuan, J.; Liu, L.; Xiao, L. Hybrid electromagnetic unified power flow controller: A novel flexible and effective approach to control power flow. IEEE Trans. Power Delivery 2018, 33, 2061–2069.

- [13] Besharat, H.; Taher, S.A. Congestion management by determining optimal location of TCSC in deregulated power systems. *Int. J. Electr. Power Energy Syst.* 2008, 30, 563–568.
- [14] Lim, J.U.; Moon, S.I. An analytical approach for the operation of series compensators to relieve power flow congestion. *Euro. Trans. Electr. Power* 2003, 13, 247–252.
- [15] Reddy, A.K.; Singh, S.P. Congestion mitigation using UPFC. *IET Gener. Transm. Distrib.* 2016, 10, 2433–2442.
- [16] Chong, B.; Zhang, X.P.; Godfrey, K.R.; Yao, K.R.; Yao, L.; Bazargan, M. Optimal location of unified power flow controller for congestion management. *Euro. Trans. Electr. Power* 2010, 20, 600–610.
- [17] Bhattacharyya, B.; Gupta, V.K. Fuzzy based evolutionary algorithm for reactive power optimization with FACTS devices. *Int. J. Electr. Power Energy Syst.* 2014, 61, 39–47.
- [18] Preedavichit, P.; Srivastava, S.C. Optimal reactive power dispatch considering FACTS devices. *Electr. Power Syst. Res.* 1998, 46, 251–257.
- [19] Dutta, S.; Mukhopadhyay, P.; Roy, P.K.; Nandi, D. Unified power flow controller based reactive power dispatch using oppositional krill herd algorithm. *Int. J. Electr. Power Energy Syst.* 2016, 80, 10–25.
- [20] Thukaram, D.; Yesuratham, G. Optimal reactive power dispatch in a large power system with AC-DC and FACTS controllers. *IET Gener. Transm. Distrib.* 2008, 2, 71–81.
- [21] Sawhney, H.; Jeyasurya, B. Application of unified power flow controller for available transfer capability enhancement. *Electr. Power Syst. Res.* 2004, 69, 155–160.
- [22] Shahraei-Ardakani, M.; Blumsack, S.A. Transfer capability improvement through market-based operation of series FACTS devices. *IEEE Trans. Power Syst.* 2016, 31, 3702–3714.
- [23] Kumar, A.; Kumar, J. ATC with ZIP load model - A comprehensive evaluation with third generation FACTS in restructured electricity markets. *Int. J. Electr. Power Energy Syst.* 2014, 54, 546–558.
- [24] Xiao, Y.; Song, Y.H.; Liu, C.C.; Sun, Y.Z. Available transfer capability enhancement using FACTS devices. *IEEE Trans. Power Syst.* 2003, 18, 305–312.
- [25] Jirapong, P.; Ongsakul, W. Optimal placement of multi-type FACTS devices for total transfer capability enhancement using hybrid evolutionary algorithm. *Electr. Power Compon. Syst.* 2007, 35, 981–1005.
- [26] Singh, J.G.; Qazi, H.W.; Ghandhari, M. Load curtailment minimization by optimal placement of unified power flow controller. *Int. Trans. Electr. Energ. Syst.* 2016, 26, 2272–2284.

- [27] Nasri, A.; Conejo, A.J.; Kazempour, S.J.; Ghandhari, M. Minimizing wind power spillage using an OPF with FACTS devices. *IEEE Trans. Power Syst.* 2014, 29, 2150–2159.
- [28] Tang, Y.; Liu, Y.; Ning, J.; Zhao, J. Multi-time scale coordinated scheduling strategy with distributed power flow controllers for minimizing wind power spillage. *Energies* 2017, 10, 1804.
- [29] Rasoulzadeh-Akhijahani, A.; Mosallanejad, A. Analyzing TCSC and SVC effects in wind power curtailment mitigation. *Int. Trans. Electr. Energ. Syst.* 2016, 26, 2445–2462.
- [30] Kapetanaki, A.; Levi, V.; Buhari, M.; Schachter, J.A. Maximization of wind energy utilization through corrective scheduling and FACTS deployment. *IEEE Trans. Power Syst.* 2017, 32, 4764–4773.
- [31] Li, S.; Ding, M.; Wang, J.; Zhang, W. Voltage control capability of SVC with var dispatch and slope setting. *Electr. Power Syst. Res.* 2009, 79, 818–825.
- [32] Varma, R.K.; Siavashi, E.M. PV-STATCOM: A new smart inverter for voltage control in distribution systems. *IEEE Trans. Sustain. Energy* 2018, 9, 1681–1691.
- [33] Liu, J.Y.; Song, Y.H.; Mehta, P.A. Strategies for handling UPFC constraints in steady state power flow and voltage control. *IEEE Trans. Power Syst.* 2000, 15, 566–571.
- [34] Sao, W.; Vittal, V. LP-based OPF for corrective FACTS control to relieve overloads and voltage violations. *IEEE Trans. Power Syst.* 2006, 21, 1832–1839.
- [35] Faried, S.O.; Billinton, R.; Aboreshaid, S. Probabilistic technique for sizing FACTS devices for steady state voltage profile enhancement. *IET Gener. Transm. Distrib.* 2009, 3, 385–392.
- [36] Liao, H.; Milanovic, J.V. On capability of different FACTS devices to mitigate a range of power quality phenomena. *IET Gener. Transm. Distrib.* 2017, 11, 1202–1211.
- [37] Goswami, A.K.; Gupta, C.P.; Singh, G.K. Minimization of voltage sag induced financial losses in distribution systems using FACTS devices. *Electr. Power Syst. Res.* 2011, 81, 767–774.
- [38] Milanovic, J.V.; Zhang, Y. Global minimization of financial losses due to voltage sags with FACTS based devices. *IEEE Trans. Power Delivery* 2010, 25, 298–306.
- [39] Enslin, J.H.R.; Zhao, J.; Spee, R. Operation of the unified power flow controller as harmonic isolator. *IEEE Trans. Power Electron.* 1996, 11, 776–784.
- [40] Rajabi-Ghahnavieh, A.; Fotuhi-Firuzabad, M.; Shahidehpour, M.; Feuillet, R. UPFC for enhancing power system reliability. *IEEE Trans. Power Delivery* 2010, 25, 2881–2890.

- [41] Zarghami, M.; Crow, M.L.; Jagannathan, S. Nonlinear control of FACTS controllers for damping interarea oscillations in power systems. *IEEE Trans. Power Delivery* 2010, 25, 3113–3121.
- [42] Du, W.; Wu, X.; Wang, H.F.; Dunn, R. Feasibility study to damp power system multi-mode oscillations by using a single FACTS device. *Int. J. Electr. Power Energy Syst.* 2010, 32, 645–655.
- [43] Pal, B.C. Robust damping of interarea oscillations with unified power-flow controller. *IEE Proc. Gener. Transm. Distrib.* 2002, 149, 733–738.
- [44] Cong, L.; Wang, Y. Co-ordinated control of generator excitation and STATCOM for rotor angle stability and voltage regulation enhancement of power systems. *IEE Proc. Gener. Transm. Distrib.* 2002, 149, 659–666.
- [45] Esparza, A.; Segundo, J.; Nunez, C.; Visairo, N.; Barocio, E.; Garcia, H. Transient stability enhancement using a wide-area controlled SVC: An HIL validation approach. *Energies* 2018, 11, 1639.
- [46] Kanchanaharuthai, A.; Chankong, V.; Loparo, K.A. Transient stability and voltage regulation in multimachine power systems vis-a-vis STATCOM and battery energy storage. *IEEE Trans. Power Syst.* 2015, 30, 2404–2416.
- [47] Mihalic, R.; Zunko, P.; Povh, D. Improvement of transient stability using unified power flow controller. *IEEE Trans. Power Delivery* 1996, 11, 485–492.
- [48] Gholipour, E.; Saadate, S. Improving of transient stability of power systems using UPFC. *IEEE Trans. Power Delivery* 2005, 10, 1677–1682.
- [49] Movahedi, A.; Niasar, A.H.; Gharehpetian, G.B. Designing SSSC, TCSC, and STATCOM controllers using AVURPSO, GSA, and GA for transient stability improvement of a multi-machine power system with PV and wind farms. *Int. J. Electr. Power Energy Syst.* 2019, 106, 455–466.
- [50] Mansour, Y.; Xu, W.; Alvarado, F.; Rinzin, C. SVC placement using critical modes of voltage instability. *IEEE Trans. Power Syst.* 1994, 9, 757–763.
- [51] Kumar, G.N.; Kalavathi, M.S. Cat swarm optimization for optimal placement of multiple UPFC's in voltage stability enhancement under contingency. *Int. J. Electr. Power Energy Syst.* 2014, 57, 97–104.
- [52] Yorino, N.; El-Araby, E.E.; Sasaki, H.; Harada, S. A new formulation for FACTS allocation for security enhancement against voltage collapse. *IEEE Trans. Power Syst.* 2003, 18, 3–10.
- [53] Gasperic, S.; Mihalic, R. The impact of serial controllable FACTS devices on voltage stability. *Int. J. Electr. Power Energy Syst.* 2015, 64, 1040–1048.

- [54] Gasperic, S.; Mihalic, R. Estimation of the efficiency of FACTS devices for voltage-stability enhancement with PV area criteria. *Renew. Sustain. Energy Rev.* 2019, 105, 144–156
- [55] Galvani, S.; Hagh, M.T.; Sarifian, M.B.B.; Mohammadi-Ivatloo, B. Multiobjective predictability-based optimal placement and parameters setting of UPFC in wind power included power systems. *IEEE Trans. Ind. Inf.* 2009, 15, 878–888.
- [56] Tripathy, M.; Mishra, S. Bacteria foraging-based solution to optimize both real power loss and voltage stability limit. *IEEE Trans. Power Syst.* 2007, 22, 240–248.
- [57] Benabid, R.; Boudour, M.; Abido, M.A. Optimal location and setting of SVC and TCSC devices using non-dominated sorting particle swarm optimization. *Electr. Power Syst. Res.* 2009, 79, 1668–1677.
- [58] Lashkar Ara, A.; Kazemi, A.; NabaviNiaki, S.A. Multiobjective optimal location of FACTS shunt-series controllers for power system operation planning. *IEEE Trans. Power Delivery* 2012, 27, 481–490.
- [59] Bhattacharyya, B.; Kumar, S. Approach for the solution of transmission congestion with multi-type FACTS devices. *IET Gener. Transm. Distrib.* 2016, 10, 2802–2809.
- [60] Kotsampopoulos, P.; Georgilakis, P.; Lagos, D.T.; Kleftakis, V.; Hatziargyriou, N. FACTS Providing Grid Services: Applications and Testing. *Energies* 2019, 12, 2554
- [61] Sullivan, D.; Mader, D. Fundamentals and Characteristics of Dynamic Reactive Power Control. In *Proceedings of the IEEE PESWebinar*, 18 December 2018.
- [62] IEEE. IEEE 1031:2011. IEEE Guide for the Functional Specification of Transmission Static Var Compensators; IEEE:Piscataway, NJ, USA, 2011.
- [63] IEEE. IEEE P1052/08. IEEE Approved Draft Guide for the Functional Specifications for Transmission Static Synchronous Compensator (STATCOM) Systems; IEEE: Piscataway, NJ, USA, 2018.
- [64] IEC. IEC 61954:2011. Static var Compensators (SVC)—Testing of Thyristor Valves; International Electrotechnical Commission: Geneva, Switzerland, 2011.
- [65] IEC. IEC 62927:2017. Voltage Sourced Converter (VSC) Valves for Static Synchronous Compensator (STATCOM)—Electrical Testing; International Electrotechnical Commission: Geneva, Switzerland, 2017
- [66] Khodaei, A., Shahidehpour, M.: 'Microgridbased co-optimization of generation and transmission planning in power systems', *IEEE T. Power Syst.*, 2013, 28, (2), pp.1582–1590
- [67] Singh, B., Chandra, A., Al-Haddad, K.: 'Unified Power Quality Compensators', In 'Power Quality Problems and Mitigation Techniques' (Wiley, 2015). pp.

- [68] Kumar, G.S., Vardhana, P.H., Kumar, B.K., Mishra, M.K.: 'Minimization of VA loading of Unified Power Quality Conditioner (UPQC)' Int. Conf. Power Eng. Energy Elect. Drives, March 2009
- [69] Han, B., Bae, B., Kim, H., Baek, S.: 'Combined operation of unified power-quality conditioner with distributed generation', IEEE Trans. Power Delivery, 2006, 21, (1), pp. 330–338
- [70] Tan, K. T., So, P.L., Chu, Y.C., Chen, M.Z.Q.: 'A flexible AC distribution system device for a microgrid', IEEE T. Energy Convers., 2013, 28, (3), pp. 601–610.
- [71] Mittapally, S.K., Pang, C., Renduchintala, U.K.: 'Mitigation of subsynchronous resonance in power grid integrated with PV power station', 2018 Int. Conf. Power Energy Environ. Intell. Control (PEEIC), Greater Noida, India, 2018, pp. 507–511.
- [72] Renduchintala, U.K., Pang C., Kumar Maddukuri S. P., Aravinthan V.: 'Fuzzy theory based distributed power flow conditioner to enhance power system dynamic stability', 2018 Int. Conf. Power Energy Environ Intell. Control (PEEIC), Greater Noida, India, 2018, pp. 1–5.
- [73] Ghosh A., Ledwich G. (2002) Unified Power Quality Conditioner. In: Power Quality Enhancement Using Custom Power Devices. The Springer International Series in Engineering and Computer Science (Power Electronics and Power Systems). Springer, Boston, MA. https://doi.org/10.1007/978-1-4615-1153-3_10
- [74] Renduchintala, U.K., Chengzong Pang, Maddukuri SVPK, Aravinthan, V., 'Smooth shunt control of a fuzzy based distributed power flow controller to improve power quality', 2016 IEEE Int. Conf. Inf. Autom. Sustain. (ICIAfS), Galle, 2016, pp. 1–5.
- [75] Wang, C., Chew, M., & Harlow, D. G. (2015). A study of membership functions on mamdani-type fuzzy inference system for industrial decision-making.
- [76] Şahin, M.; Erol, R. A Comparative Study of Neural Networks and ANFIS for Forecasting Attendance Rate of Soccer Games. Math. Comput. Appl. 2017, 22, 43.
- [77] McCullagh, J. Data mining in sport: A neural network approach. Int. J. Sports Sci. Eng. 2010, 4, 131–138.
- [78] Maszczyk, A.; Zając, A.; Ryguła, I. A neural network model approach to athlete selection. Sports Eng. 2011, 13, 83–93
- [79] Renduchintala, U.K., Pang, C., Pavan, S.V., Maddukuri, K., Tatikonda, K.M.: 'Comparison of MPPT techniques for SEPIC converter based photovoltaic system', 2016 Online Int. Conf. Green Eng Technol. (IC-GET), Coimbatore, 2016, pp. 1–5
- [80] Mokhtarpour, A., Bathaee, M., Shayanfar, H.A.: 'Power quality compensation in smart grids with a single phase UPQC-DG', 2nd Iranian Conf. Smart Grids (ICSG), 2012

- [81] Khadkikar, V. 'Enhancing electric power quality using UPQC: a comprehensive overview', IEEE T. Power Electr., 2012, 27, (5), pp. 2284–2297
- [82] Maddukuri, SVPK, Visvakumar, A., Renduchintala, U.K.: 'An intelligent closed loop single-switch DC/DC converter with high voltage step-up ratio for roof-mounted solar cells electric vehicle', 2016 IEEE Int. Conf. Power Elect. Drives Energy Syst. (PEDES), Trivandrum, 2016, pp. 1–6.
- [83] Pourhossein, J., Gharehpetian, G.B., Fathi, SH: 'Unified interphase power controller (uipc) modeling and its comparison with IPC and UPFC', IEEE T. Power Deliver., 2012, 27, (4), pp. 1956–1963
- [84] Ye, J., Gooi H.B., Wu F.: 'Optimal design and control implementation of upqc based on variable phase angle control method', IEEE T. Ind. Inform., 2018, 14, (7), pp. 3109–3123
- [85] Han, B., Bae, B., Kim, H., Baek, S.: 'Combined operation of unified power quality conditioner with distributed generation', IEEE T. Power Deliver., 2006, 21, (1), pp. 330–338
- [86] Reddy G.S.: 'Feasibility analysis of DGSC-UPQC', Int. J. Res. Rev. Appl. Sci., 2010, 4, (1), pp. 32–47
- [87] Hosseinpour, M., Rezapour, Y.M., Torabzade, S.: 'Combined operation of unifier power quality conditioner and photovoltaic array', J. Appl. Sci., 2009, 9, (4), pp. 680–688
- [88] Renduchintala, U.K., Chengzong, P.: 'Neuro-fuzzy based UPQC controller for Power Quality improvement in micro grid system', 2016 IEEE/PES Transm. Distrib. Conf. Expo. (T&D), Dallas, TX, USA, 2016, pp. 1–5
- [89] MATLAB: Fuzzy Logic Toolbox User's Guide, Available at: <https://books.google.com/books?id=kkbvoQEACAAJ>
- [90] Malekpour AR, Pahwa A.: 'Radial test feeder including primary and secondary distribution network', 2015 North American Power Symposium (NAPS), Charlotte, NC, 2015, pp. 1–9
- [91] IEEE Std 519-1992, 'IEEE Recommended Practices and Requirements for Harmonic Control in Electric Power Systems', Institute of Electrical and Electronics Engineers, Inc. 1993.